Pathological study on the mechanism of brain damage after experimental transient hypoglycemic coma

一過性の低血糖性昏睡誘発後に生じる脳傷害の
メカニズムに関する病理学的研究

The United Graduate School of Veterinary Science

Yamaguchi University

Nagi Tomita

September 2020

ABSTRACT

Pathological Study on the Mechanism of Brain Damage after Experimental Transient Hypoglycemic Coma

Nagi Tomita

Hypoglycemic coma causes brain damage including neuronal death, which results in neurological symptoms such as a cognitive impairment, but due to its unclear pathogenesis, preventive methods have not been established. In this study, we focused on events other than neuronal death that occur in the rat brain in response to hypoglycemia, such as white matter degeneration and inflammatory response.

Inflammation plays a role in neuronal necrosis in response to hypoglycemic coma; however, the dynamics of inflammatory response including microglial activation and cytokine expression remain unclear. In this study, we aimed to elucidate the time course and distribution of morphological changes of microglia and cytokine expression in response to transient hypoglycemic coma in the rat cerebral cortex. We found that necrotic neurons appeared in the neocortex as early as 3 h after

hypoglycemic coma. Necrotic neurons were not observed in the cingulate cortex. The necrotic neurons were observed 1 day after hypoglycemic coma in the specific areas of the neocortex. Rod-shaped microglia with long dendrites were detected 3–6 h after hypoglycemia corresponding to the extent of the neuronal necrosis. Rod-shaped microglia were rarely observed from days 1 to 14; instead there was a prominent infiltration of hypertrophic and ameboid-shaped microglia. The mRNA expression of TNFα significantly increased in the neocortex at 3–6 h after hypoglycemic coma compared to the controls, while in the cingulate cortex, it significantly increased at 3 h only. Our results indicate that early and transient appearance of rod-shaped microglia and persisting of high expression level of TNFα are characteristic observations in inflammatory response to hypoglycemic neuronal damage in the cerebral neocortex, which might contribute to neuronal necrosis in response to transient hypoglycemic coma.

Patients with hypoglycemic coma exhibit abnormal signals in the white matter on magnetic resonance imaging. Further, the distribution of the abnormal signals had association with the patients' short-term outcomes. However, precise pathological changes in the white matter caused by hypoglycemia remain unclear in humans and experimental animals. We aimed to reveal the distribution and time

course of histopathological and immunohistochemical changes occurring in the white matte during the early stages of transient experimental hypoglycemic coma. Histologically, edema was observed in the fiber bundles of the globus pallidus from the brains obtained days 1–14. Additionally, myelin pallor and a decrease in neurofilament 200 kDa-positive signals were observed on day 14. Microglial infiltration to the fiber bundles and astrogliosis were also detected. Observations similar to the globus pallidus, except for edema, were also noted in the internal capsule. In the corpus callosum, a mild decrease in neurofilament-positive signals, microgliosis, and astrogliosis were observed. These results suggest that after transient hypoglycemic coma, edema and/or degeneration occurred in the white matter, especially in the globus pallidus, internal capsule, and corpus callosum in the early stages.

TABLE OF CONTENTS

CHAPTER 2: Histopathological and immunohistochemical analyses of the cerebral white matter after insulin-induced hypoglycemic coma

GENERAL INTRODUCTION AND BACKGROUND

1. Social impact of hypoglycemia

Hypoglycemia occurs in patients with insulin-producing tumor, or with diabetes under strict restriction of blood glucose. Hypoglycemia is not an uncommon event for diabetic patients who are treated with insulin and/or other drugs (Ben-Ami et al.,1999; Donnelly et al., 2005). Previous reports demonstrate that insulin-treated patients with type 1 diabetes experience at least one severe hypoglycemia episode per patient per year (Pramming et al., 1999; ter Braak et al., 2000; Donnelly et al., 2005). Severe hypoglycemic coma causes neuronal death that is occasionally accompanied by neurological symptoms such as cognitive impairment (Auer et al., 1989; Languren et al., 2013). However, methods for preventing hypoglycemic brain damage have not been established. The clinical practice guidelines for hypoglycemia focus on the methods for recovery of the blood glucose level, while they do not mention the methods for preventing the possible brain damage following severe hypoglycemia (Clayton et al., 2013). The International Diabetes Foundation estimates that the number of people with diabetes will increase by approximately 1.5-fold in a few decades (Cho et al., 2018). Therefore, concern regarding hypoglycemia is rising along with growing population of diabetic patients and the

development of new strategies for the prevention and/or treatment of hypoglycemic brain damage is becoming an important task.

2. Hypoglycemic coma-induced neuronal death

Brain damage in response to hypoglycemic coma is characterized by neuronal death in specific brain regions such as the Cornu Ammonis 1 (CA1) of the hippocampus, dentate gyrus, subiculum, cerebral cortex, and caudate and putamen in experimental animals and humans (Auer et al., 1984a; Auer et al., 1984b; Auer et al., 1989; Mori et al., 2010). However, precise pathogenesis of neuronal death after hypoglycemia remains unclear. In those brain regions, the morphology of neurons or biochemistry in response to hypoglycemic coma have been reported finely in old experimental studies; however the prior studies have focused on how to decrease the neuronal death in gray matter, whereas they have ignored damage in white matter (axons, myelin) and glial cell reactions in response to hypoglycemic coma.

OBJECTIVE AND STRUCTURE OF THE THESIS

We aimed to redefine the mechanism of hypoglycemic brain damage by focusing on other factors than neuronal death, which may contribute to the development of new strategies for the prevention and/or treatment of hypoglycemic brain damage. Therefore, in the present study, we focused on events other than neuronal death that occur in brain in response to hypoglycemic coma, such as a glial cell activation and white matter degeneration.

In chapter 1: To reveal the time course of inflammatory response including microglial activation and cytokine expressions following transient hypoglycemic coma by morphological and molecular analysis of the rat cerebral cortex and to define the role of microglial cells in hypoglycemic neuronal damage

In chapter 2: To reveal the distribution and time course of histological and immunohistochemical findings in the white matter in response to transient hypoglycemic coma.

LIST OF ORIGINAL PUBLICATIONS

The thesis is based on the following original publications.

Nagi Tomita, Tomoki Nakamura, Yuji Sunden, Takehito Morita (2020).

Histopathological and immunohistochemical analysis of the cerebral white matter after transient hypoglycemia in rat.

The Journal of Veterinary Medical Science 82(1), 68–76.

Nagi Tomita, Tomoki Nakamura, Yuji Sunden, Hajime Miyata, Takehito Morita (2020).

Temporal analysis of histopathology and cytokine expression in the rat cerebral cortex after insulin-induced hypoglycemia.

Neuropathology In press

CHAPTER 1

Histopathology and cytokine expression in the cerebral cortex after insulin-induced hypoglycemic coma

ABSTRACT

Inflammation plays a role in neuronal necrosis in response to hypoglycemic coma; however, the dynamics of inflammatory response including microglial activation and cytokine expression remain unclear. In this study, we aimed to elucidate the time course and distribution of morphological changes of microglia and cytokine expression in response to hypoglycemic coma in the rat cerebral cortex. Rats were provided an insulin-induced hypoglycemic coma followed by recovery as described above. Rat brains were collected after 3, 6, and 24 h and after 3, 5, 7, and 14 days. We performed histopathological analysis and immunohistochemical analysis using primary antibodies for Iba-1, neuronal nuclei (NeuN), GFAP in the cingulate cortex and four areas of the neocortex: hindlimb (HL), parietal cortex area 1 (Par1), parietal cortex area 2 (Par2) and perirhinal cortex (PRh). Real-time reverse transcriptase-polymerase chain reaction was used to measure tumor necrosis factor alpha (TNF α) and interleukin-6 mRNA expression in the cingulate cortex and neocortex. We found that necrotic neurons appeared in all four areas in the neocortex as early as 3 h after hypoglycemic coma. Necrotic neurons were not observed in the cingulate cortex. The number of NeuN-immunopositive neurons decreased 1 day after hypoglycemic coma in the HL, Par2, and PRh areas. In Iba-1 immunostaining, rod-shaped microglia with long dendrites were

detected 3–6 h after hypoglycemia, and commonly observed in the HL, Par2, and PRh areas. Rod-shaped microglia were rarely observed from days 1 to 14; instead there was a prominent infiltration of hypertrophic and ameboid-shaped microglia. The mRNA expression of TNF α significantly increased in the neocortex at 3–6 h after hypoglycemic coma compared to control animals, while in the cingulate cortex it significantly increased at 3 h only. Our results indicate that early and transient appearance of rod-shaped microglia and persisting high expression level of TNF α are characteristic observations in inflammatory response to hypoglycemic neuronal damage in the cerebral neocortex, which might contribute to neuronal necrosis in response to transient hypoglycemic coma.

INTRODUCTION

The cerebral neocortex, hippocampus, caudate and putamen are some of the regions of the brain where neuronal necrosis is typically recognized after severe hypoglycemia in experimental animals and human cases (Auer et al., 1984a; Auer et al., 1984b; Auer et al., 1989; Mori et al., 2006; Won et al., 2012; Brown et al., 2015). In those cases, diffuse neuronal necrosis was observed in the cerebral neocortex lamina 2 and 3, while the adjacent surface of the cingulate cortex and the deeper layers of the neocortex were mostly spared (Auer et al., 1984b).

A detailed pathogenesis of neuronal death in response to hypoglycemia remains unclear. Factors such as excitotoxicity and apoptotic mechanisms have been reported to contribute to neuronal death in severe hypoglycemia (Languren et al., 2013). A recent study demonstrated that excessive activation of microglia was a factor aggravating neuronal death caused by severe hypoglycemia (Won et al., 2012). In that study, hypoglycemia-induced neuronal death and microglial activation in the Cornu Ammonis 1 of the hippocampus were reduced by intra-peritoneal injection of minocycline, an anti-inflammatory agent. It has also been reported that microglial activation contributes to the pathogenesis of acute neuronal diseases such as stroke and trauma, neurodevelopmental

diseases such as autism, and neurodegenerative diseases such as multiple sclerosis, Alzheimer's disease and Parkinson's disease (Brown et al., 2015; Salter et al. 2017). Microglia exhibit dynamic morphological changes when they are activated, and their morphology indicates their functions or activated states (Stence et al., 2001; Kettenmann et al., 2011); for example, ameboid-shaped microglia exhibit a high capability for phagocytosis or locomotion with the expression of many activated markers (Raivich et al., 1999; Stence et al., 2001; Kettenmann et al., 2011). However, the dynamics of microglial activation including their morphological changes in response to hypoglycemia are unknown. Therefore, it is important to investigate the temporal progression of microglial activation morphologically after severe hypoglycemia to reveal the role of microglia in neuronal damage caused by transient hypoglycemia.

Under pathological conditions, activated microglial cells can be sources of cytokines such as tumor necrosis factor alpha (TNFα) and interleukin-6 (IL-6). TNFα and IL-6 are proinflammatory cytokines that are induced during the early stage of brain damage to initiate an inflammatory response (Bruce et al., 1996; Raivich et al., 1999; Hanisch et al., 2002). At present, no studies have reported on the dynamics of cytokines in the brain following hypoglycemic brain damage. In the present study, we analyzed the mRNA expression of TNFα and IL-6 in the rat cerebral cortex to assess inflammatory

response to transient hypoglycemic coma.

We aimed to reveal the time course of inflammatory response including microglial activation and cytokine expressions following transient hypoglycemic coma by morphological and molecular analysis of the rat cerebral cortex and to define the role of microglial cells in hypoglycemic neuronal damage. Our findings may contribute to the development of new strategies for the prevention and/or treatment of hypoglycemic brain damage.

.

MATERIALS AND METHODS

Animals

Six-week-old male Sprague-Dawley rats (210–310 g) were purchased from Clea Japan, Inc. (Tokyo, Japan). All protocols in this study were approved by the Animal Research Committee and performed in accordance with the guidelines for animal experiments of the Faculty of Agriculture, Tottori University (Tottori, Japan).

Hypoglycemic treatment

Prior to the experiments, the rats were fasted overnight, with access to only tap water. On the following day, the animals were intra-peritoneally injected with 3.5–5.0 U/kg body weight of regular insulin (Novolin R, Novonordisk, Tokyo, Japan) to induce hypoglycemic coma. Blood samples were collected from the caudal vein and blood glucose levels were measured with a glucometer (Antsense III, HORIBA, Kyoto, Japan) every 30 min until 6 h post-insulin administration. One final blood sample was collected at 24 h post-insulin administration. Body temperatures were measured every hour until 6 h post-insulin administration on representative rats (weighing environment logger, A&D Company, Ltd., Tokyo, Japan). The rats were anesthetized with 2–5% isoflurane (Intervet, Tokyo,

Japan) in an anesthesia apparatus (DS Pharma Co., Ltd., Osaka, Japan) during the blood sampling and body temperature measurements. The onset of coma in severe hypoglycemia was determined by low blood glucose levels (< 21 mg/dl), absence of reaction to external stimuli, and loss of corneal reflection. The coma state was maintained for 15–30 min. Subsequently, the rats were intra-peritoneally injected with 50% glucose (0.5–1.5 ml) followed by frequent injections of a 1:1 mixture of 50% glucose and Krebs-Henseleit buffer (0.1–0.5 ml per injection; total of 1–3.5 ml) for 4 h to terminate the hypoglycemic coma. As a control, sham-hypoglycemic rats were given insulin (3.5 U/kg) and glucose injections simultaneously to maintain euglycemia. After recovery, all rats were given free access to tap water and food pellets (Clea Japan, Inc.) and kept until they were killed. Clinical signs were monitored throughout the hypoglycemic treatment and recovery period until the rats were killed. The blood glucose levels were expressed as means of representative animals (n= 2) in each group.

Tissue preparation for histology and immunohistochemistry

The rats were killed after 3, 6, and 24 h and 3, 5, 7, and 14 days post-hypoglycemia (n= 2–7 per group). The sham-hypoglycemic rats were killed at 7 days post-hypoglycemia (n= 3). First, the animals were deeply anesthetized by intra-peritoneal injection of

pentobarbital sodium (64.8 mg/kg; Kyoritsu Seiyaku, Tokyo, Japan) and inhalation of 2–5% isoflurane. Then they were intra-aortically perfused with 100 ml saline to wash the blood vessels, followed by 300 ml of 10% neutral phosphate-buffered formalin. The brains were removed soon after perfusion and sectioned coronally into 1.5-mm thick slices; two of the sections (Bregma -1.8 mm and -3.3 mm) were prepared for histological and immunohistochemical analyses. The brain sections were fixed with 10% neutral phosphate-buffered formalin again, immersed in ethanol and xylene, and then embedded in paraffin. Four-μm thick sections were cut from each tissue block for hematoxylin and eosin (HE) staining and immunohistochemistry.

Immunohistochemical procedure

After deparaffinization, the brain sections were transferred into citric acid buffer (pH 6.0) and boiled for 15 min at 98°C in a microwave processor (MI-77, Azuma, Tokyo, Japan) to retrieve antigens. Endogenous peroxidase activity was blocked with 3% hydrogen peroxide for 15 min, and the sections were pre-incubated with 10% normal goat serum for 30 min at room temperature. After that, the sections were incubated with a rabbit polyclonal anti- Iba-1 antibody (diluted 1:2000, Wako, Osaka, Japan), mouse monoclonal anti-neuronal nuclei (NeuN) antibody (EMD Millipore corp., Burlington,

MA, USA), and anti- GFAP antibody (diluted 1:100, Dako Denmark A/S, Glostrup, Denmark) at 4 ° C overnight. The reaction was revealed using 3, 3'-diaminobenzidine tetra-hydrochloride as a chromogen (Agilent, Tokyo, Japan) and counterstaining was performed with hematoxylin.

Assessment of NeuN-positive neurons

Assessment of NeuN-positive cells was performed at 1 and 14 days after hypoglycemia and in the sham-hypoglycemic controls (n= 3, 5, and 3, respectively). An Olympus BX51 microscope equipped with an Olympus D21-HS digital camera was used for image acquisition. The number of NeuN-positive cells that located in lamina 2 and 3 within an entire 20× image frame was counted. Neurons were judged to be positive for NeuN when they exhibit weak to strong positive signals in the nuclei and/or cytoplasm. Ten frames per rat were analyzed. Each image was taken in five areas of the cerebral cortex: the retrosplenial agranular cortex in the cingulate cortex, hindlimb area (HL), parietal cortex area 1 (Par1), parietal cortex area 2 (Par2), and perirhinal cortex (PRh) of both hemispheres. Cell counts were reported as the sum of both hemispheres in each brain area.

Assessment of microglial cell morphology

Assessment of Iba-1-positive cells was performed in animals at 3 and 6 h, and 5, 7, and 14 days post-hypoglycemia and in sham-hypoglycemic controls (n= 4, 2, 2, 2, 4, and 3, respectively). A microscope equipped with a digital camera was used for image acquisition. The number of Iba-1-positive cells within an entire 40× image frame was counted; we analyzed five frames per animal. Each image was taken in five areas of the cerebral cortex (cingulate cortex, HL, Par1, Par2, PRh) of the right hemisphere. All images were from lamina 2 to 3 of the cerebral cortex. Iba-1-positive cells were sorted into four subtypes depending on previously published morphological characteristics: 1) ramified-shaped cells with delicate dendrites and small, round to ovoid nuclei with thin cytoplasm, 2) hypertrophic cells with shorter and thicker dendrites and slightly swollen cell bodies, 3) ameboid-shaped cells with no or few retracted dendrites and irregular cell bodies, 4) rod-shaped cells with long bipolar dendrites and slender cell bodies with round to rod-shaped nuclei (Ziebell et al., 2012; Taylor et al., 2014; Wyatt-Johnson et al., 2017). The cell counts from five frames were aggregated to obtain the total cell counts. The three time intervals of the neocortex were 3 and 6 h post-hypoglycemia (n= 6), 5 and 7 days post-hypoglycemia (n= 4), and 14 days post-hypoglycemia (n= 4). Data of the cingulate cortex included those of animals at 3 and 6 h and 5, 7, and 14 days post-hypoglycemia

(n= 14).

The detailed distribution of rod-shaped cells in the cerebral cortex was examined in animals at 3 and 6 h post-hypoglycemia (n= 4 and 2, respectively). Each rod-shaped cells was plotted as a dot on a brain map of the coronal section (Bregma -3.3 mm) for each animal. The brain maps of all animals were merged to form one brain map.

Assay of cytokines

The RNA levels of IL-6 and TNFα were analyzed in the hypoglycemic and sham-hypoglycemic rats. The animals were killed at 3 and 6 h post-hypoglycemic coma (n= 4 per group). Sham-hypoglycemic rats were killed at 8 h post-insulin injection (approximately 6 h post sham-hypoglycemia). Animals were deeply anesthetized as described above, and then intra-aortically perfused with 100 ml saline to wash the blood vessels, decapitated, and the brains were removed immediately. The brains were sectioned coronally into 2-mm thick slices. In one of the sections (Bregma -1.8 mm to -3.8 mm), tissues of the PRh area around the rhinal fissure and the cingulate cortex of both hemispheres were frozen in liquid nitrogen and stored until RNA extraction and reverse transcription-polymerase chain reaction (RT-PCR). Total RNA was extracted from the neocortex and the cingulate cortex of rats after hypoglycemic coma or sham-hypoglycemia

using the RNeasy Plus Universal Mini Kit (Qiagen, Hilden, Germany) according to the manufacturer's instructions. The extracted RNA (760 ng) was used for the reverse-transcription and cDNA synthesis using the Primer Script™ II High Fidelity RT-PCR Kit (Takara Bio, Shiga, Japan) according to the manufacturer's instructions. The reverse-transcription reaction was performed with a T100™ Thermal Cycler (Bio Rad Laboratories, Hercules, CA, USA). Subsequently, the cDNA was used for real time polymerase chain reaction (PCR) with the SsoAdvanced™ Universal SYBR Green Supermix (Bio Rad Laboratories) according to the manufacturer's instructions. Real time PCR was carried out with the CFX Connect™ Real-Time System (Bio Rad Laboratories). The cycle of threshold values of each target gene expression level of the samples was normalized to the expression level of the housekeeping gene β-Actin. The expression level of each gene was recorded as a relative value versus the sham-hypoglycemic control calculated by the $2^{-\Delta\Delta CT}$ value. The following primer sequence were used (5' to 3', forward/reverse):

TNFα (TGATCGGTCCCAACAAGGA/TGCTTGGTGGTTTGCTACGA); IL-6 (TCCTACCCCAACTTCCAATGCTC/TTGGATGGTCTTGGTCCTTAGCC);

β-actin (CCCCATTGAACACGGCATT/CATCTTTTCACGGTTGGCCTTA).

Statistical analysis

Data are expressed as mean ± SEM except for the blood glucose levels. Data on the number of Iba-1-positive cells in the neocortex or NeuN-positive cells were assessed by one-way ANOVA followed by Dunnett's test for comparisons of multiple groups against a control group. Data on the number of Iba-1 positive cells in the cingulated cortex were assessed using the two-sample, two-tailed Student's t-test. Data on the mRNA levels of cytokines were assessed by one-way ANOVA followed by Tukey's HSD test to make multiple pairwise comparisons between groups. P-values < 0.05 were considered statistically significant.

RESULTS

Clinical observation of animals

Rats exhibited symptoms of severe hypoglycemia when blood glucose levels dropped below 20 mg/dl and subsequently went into a coma (Fig. 1). Typically, the onset of the coma occurred within 2–3.5 h after administration of insulin injection. All rats quickly recovered consciousness after administration of glucose injection. Blood glucose levels increased and reached the pre-insulin injection levels within 3 h after administration of glucose injection. Rats with sham-hypoglycemia exhibited only a minimal decrease of the blood glucose, and the blood glucose levels were maintained above 60 mg/dl. The rats showed no significant changes in the breathing rate and body temperature during hypoglycemia and recovery. There were no significant neurological symptoms throughout the survival period following hypoglycemic treatment.

Histopathology

Necrotic neurons with shrunken, acidophilic cytoplasm and pyknotic nuclei were observed in cerebral neocortex lamina 2 and 3 as early as 3 h and up to 14 days after hypoglycemic coma (Fig. 2). Such acidophilic neurons were scattered at 3 and 6 h, and

the most severe cases were observed from days 1–7 post-hypoglycemic coma. At day 14, the acidophilic neurons exhibited highly indistinct cell body and nuclear outlines and were difficult to detect; some were surrounded by microglia-like cells. Edema was observed around the acidophilic neurons or capillaries and in neuropils of lamina 2 and 3 from 3 h to 3 days post-hypoglycemia. Acidophilic neurons were not detected in the cingulate cortex and rarely detected in the deeper layers of the neocortex. Sham-hypoglycemic rats did not exhibit acidophilic neurons in any areas of the cerebral cortex.

Immunohistochemistry

Assessment of NeuN-positive neurons

Neurons exhibiting NeuN-positive nuclei and cytoplasm were densely present in lamina 2 and 3 of the neocortex and the cingulate cortex of control animals (Fig. 3A). Neurons with shrunken, acidophilic cytoplasm, and pyknotic nuclei in HE staining were negative to minimally positive for NeuN in the cytoplasm and NeuN-negative in the nuclei (Fig. 3B, inset). As the shrunken NeuN-negative neurons increased, NeuN-positive neurons were scattered in lamina 2 and 3 and the positive signals were weaker than those of control animals (Fig. 3B). Neurons that appeared to be intact in HE staining occasionally exhibited a decrease of NeuN-positive signals from 3 h to 14 days after

hypoglycemia. They exhibited negative to weak NeuN positivity in the cytoplasm and weak to strong NeuN positivity in the nuclei. Such neurons were observed not only in the superficial layers (lamina 2 and 3) of the neocortex but also in the deeper layers (lamina 4–6).

The number of NeuN-positive cells in lamina 2 and 3 decreased significantly in the HL, Par2 and PRh areas of the neocortex 1 day after hypoglycemia (Fig. 4). A significant decrease in the number of NeuN-positive cells was observed only in the PRh 14 days after hypoglycemia. A significant decrease in the number of NeuN-positive cells was not observed in the cingulate cortex.

Assessment of morphology in microglia

In control animals, most of Iba-1-positive cells were spread evenly and exhibited a ramified shape with fine and highly branched dendrites and small cell bodies (Fig. 5A, B). Rod-shaped cells observed in lamina 2 and 3 from 3 h and up to 6h post-hypoglycemia (Fig. 5C). They had long (maximum 200 μm), straight dendrites with side branches that often run parallel to neuronal axons, or completely wrapped dendrites and/or cell bodies of neurons (Fig. 5D). They occasionally had tiny and clear vacuoles in the cytoplasm. Rod-shaped cells were rarely observed after 1 day of hypoglycemia. Hypertrophic cells

which have shorter and thicker dendrites appeared not only in the surface layers (lamina1-3), but also in the deeper layers (lamina 4-6) at 3 h and 6 h post-hypoglycemia (Fig. 5E). Hypertrophic cells occasionally had tiny and clear vacuoles in the cytoplasm. Ameboid-shaped cells were sometimes observed mainly in lamina 2 and 3 at 3h and 6 h post-hypoglycemia. Ameboid-shaped cells exhibited no dendrites or retracted dendrites and round- to irregularly shaped cell bodies (Fig. 5F). The number of hypertrophic and ameboid-shaped cells gradually increased in the surface layers from 1 to 7 days and was significant at 5 and 7 days post-hypoglycemia (Fig. 5G). Microglial node-like structures composed of a few ameboid cells were observed in the superficial layers from days 3 to 14, indicating phagocytosis of damaged neurons. After day 3, hypertrophic and ameboid cells were focally infiltrated in the surface layers but rarely seen in the deeper layers.

The number of Iba-1-positive cells in lamina 2 and 3 was quantified (Fig. 6). At 3–6 h, the number of rod-shaped cells in the neocortex increased significantly while the number of ramified-shaped cells decreased compared to the controls. At days 5–7 after hypoglycemia, the number of hypertrophic cells increased significantly in the neocortex. Also, the number of ameboid cells increased although the difference was not statistically significant. The number of ramified-shaped cells decreased and rod-shaped cells were rarely observed in the neocortex at days 5–7 post-hypoglycemia. The number of

hypertrophic and ameboid-shaped cells tended to increase at day 14, although the difference was not statistically significant. The number of ramified cells also decreased significantly at day 14 post-hypoglycemia.

The distribution of rod-shaped cells in the cerebral cortex was examined at 3 h and 6 h after hypoglycemia (Fig. 7). They were often found in the superficial layers of the HL, Par2, and PRh areas but rarely seen in the deeper layers of the neocortex or the cingulate cortex. The Par1 area of the neocortex exhibited a relatively sparse distribution of rod-shaped microglia compared to other areas of the neocortex.

Assessment of GFAP-positive astrocytes

GFAP-positive astrocytes were spread evenly and exhibited fine, radial dendrites, and sparse cytoplasm of the cell body in control animals. In contrast to early activation of microglia, GFAP-positive astrocytes did not exhibit activated morphology until 1 day after hypoglycemic coma, while a moderate increase of GFAP-positive signals was observed in the glial limiting membrane on the brain surface or around blood vessels 1 day after hypoglycemia. At 3 days after hypoglycemia, astrocytes exhibited moderately thickened dendrites in lamina 1–5 and pairing nuclei in lamina 1–3. In addition, astrocytes with abundant cytoplasm were occasionally seen in lamina 2 and 3 from 5 days post-

hypoglycemia onward, while there were no significant changes in the deeper layers.

Cytokine assay

The mRNA level of TNFα significantly increased in both the cingulate cortex and neocortex at 3 h, and only in the neocortex at 6 h post-hypoglycemia (Fig. 8A, B). In contrast, the levels of IL-6 mRNA were not significantly higher in any brain regions or at any time-points (Fig. 9A , B).

DISCUSSION

We found that rod-shaped microglia transiently appeared in lamina 2 and 3 of the neocortex, 3 to 6 h after hypoglycemia. In addition, the distribution of rod-shaped microglia was consistent with the extent of significant decrease in NeuN-positive neurons. Rod-shaped microglia are associated with a variety of disease conditions in experimental animals or humans, including traumatic brain injury, ischemia, status epilepticus, subacute sclerosing panencephalitis and HIV encephalitis (Graeber et al., 1994; Lambertsen et al., 2011; Ziebell et al., 2012; Wyatt-Johnson et al., 2017). In those animal models of global ischemia, trauma, and epilepsy, rod-shaped microglia were observed from one or several days and up to a few weeks after the incidence, while the dentate gyrus of rat after statue epilepticus exhibited transient appearance of rod-shaped microglia in the early phases. In our results, rod-shaped microglia were observed transiently in very early phases (3–6 h) after hypoglycemia; this finding might be characteristic to microglial activation in response to hypoglycemic coma in the cerebral neocortex. Despite their association with many diseases, the role of the rod-shaped microglia remains unclear. A previous report indicated that preservation of tissue structure is an important determinant for the formation of rod-shaped microglia (Graeber et al., 1994). When there was extensive tissue

necrosis, only phagocytic microglia could be observed. In addition, rod-shaped microglia wrapped along neuronal surface membranes including axons, apical dendrites, and cell bodies regardless of disease etiology (Graeber et al., 1994; Wirenfeldt et al., 2009; Graeber et al., 2010; Ziebell et al., 2012). Such microglia displace synaptic input, a phenomenon known as synaptic stripping, which is considered as a process for neuronal recovery. These findings suggest that rod-shaped microglia may contribute to the recovery of damaged but surviving neurons.

Immediately after hypoglycemia followed by glucose injection, neurons begin to exhibit degenerative changes and in 4–12 h, some go into recovery and others go into irreversible change (Auer et al., 1985). The time course of the appearance of rod-shaped microglia in our study parallels the time point when degenerated neurons could begin to recover. Therefore, rod-shaped microglia may be associated with the recovery of neurons that survived hypoglycemic coma in lamina 2 or 3 of the neocortex. After rod-shaped microglia, a predominant infiltration of hypertrophic or ameboid microglia is observed from 1 to 14 days after hypoglycemia. Activated microglia exhibit retraction of the dendrites and become hypertrophic, eventually exhibiting no dendrites and becoming ameboid in shape with high phagocytotic activity (Graeber et al., 2010; Wyatt-Johnson et al., 2017). In the present study, the infiltration of hypertrophic or ameboid microglia suggests

phagocytosis of irreversibly damaged neurons.

It remains unclear how the microglial activation was triggered in the present study. Excitotoxicity is a contributing factor in hypoglycemic neuronal damage (Auer et al., 2004; Languren et al., 2013). It has been shown that hypoglycemic coma causes a prominent increase of aspartate and glutamate in brain tissues and/or extracellular fluid (Norberg et al., 1976; Sandberg et al., 1986; Auer et al., 2004). Aspartate and glutamate can directly cause microglial activation with the release of TNFα through the N-methyl-D-aspartate receptor localized on microglia, while also they could cause neuronal damage as excitotoxins (Traynelis et al., 2010; Murugan et al., 2011; Murugan et al., 2013). More recently, zinc release from nerve terminals has been recognized after hypoglycemia (Suh et al., 2004). For microglia, zinc has been identified as a trigger for activation *in vivo* and in an animal model of ischemia (Kauppinen et al., 2008). Therefore, microglial activation following hypoglycemic coma can occur not only as a reaction to neuronal damage, but also as a reaction to hypoglycemia itself through factors such as excitatory amino acids or zinc.

We found that the mRNA level of TNFα in the neocortex was significantly higher than in the cingulate cortex 6 h after hypoglycemic coma. TNFα exerts pleiotropic effects on neurons and glial cells. Increased TNFα could be harmful for neurons when it

enhances edema or inflammation to an excessive degree (Brown et al., 2015; Hanisch et al., 2002). In our study, the appearance of rod-shaped microglia in the neocortex paralleled the time points when the mRNA levels of TNFα were relatively higher than in control animals. Activated microglia can be the main source of TNFα under pathological conditions including the early phase of excitotoxic neuronal damage, brain injury or oxygen-glucose deprivation (Acarin et al., 2000; Hanisch et al., 2002; Du et al., 2017). Therefore, the increase of TNFα expression and the activation of microglia recognized as morphological changes to rod, hypertrophic or ameboid-shapes may aggravate neuronal damage and death in response to hypoglycemic coma. However, the source of TNFα is uncertain in our results; therefore, we need further investigations of the localization of cytokines, as well as confirming protein expression of cytokines by Western blotting. We observed an increase of TNFα also in the cingulate cortex at 3 h after hypoglycemia, without morphologically damaged neurons or activated microglia, though the reason remains unclear.

In contrast to TNFα, the mRNA level of IL-6 did not increase in the neocortex or the cingulate cortex 3 or 6 h after hypoglycemic coma. Morphologically, an obvious activation of astrocytes was not detected from 3 h to 1 day, and only appeared gradually from 3 days after hypoglycemic coma. IL-6 is a cytokine that belongs to a family of neurokine and

known as an early marker for tissue damage in brain pathology (Raivich et al., 1999). IL-6 strongly induces activation of astrocytes through receptors localized on astrocytes but not microglia (Raivich et al., 1999). The absence of IL-6 elevation at early time-points might contribute to the delayed activation of astrocytes after hypoglycemic coma.

The number of NeuN-positive cells in lamina 2 and 3 decreased significantly in the HL, Par2, and PRh areas 1 day after hypoglycemia, while it was observed in the PRh area only at day14. The results of the present study suggest that the decrease in the number of NeuN-positive neurons after hypoglycemic coma is partly a reversible change such as neuronal degeneration, rather than neuronal death in the HL and Par 2 areas. Consistent with our findings, there are some reports demonstrating reversible decrease of NeuN-immunoreactivity after neurological incidents such as ischemic brain damage or peripheral nerve injury (McPhail et al., 2004; Ünal-Çevik et al., 2004). In those reports, it was concluded that decrease of NeuN-immunoreactivity could occur due to decrease in NeuN protein expression or loss of NeuN antigenicity.

In the present study, we used non-diabetic animals to assess the effect of hypoglycemia to the rat brain without other possible factors such as hyperglycemia or hyperlipidemia. A previous study of hypoglycemic brain damage using diabetic and non-diabetic rat demonstrated that diabetic rats exhibited more severe neuronal necrosis than

non-diabetic rats, especially in the cerebral neocortex (Bree et al., 2009). In addition, the presence of diabetes and associated hyperglycemia aggravate the neuronal damage in response to other pathological incidents such as stroke, in both preclinical and clinical cases (Lin et al., 1998; Baird et al., 2003; Moreira et al., 2007). Therefore, we should investigate cytokine expression and microglial activation in response to hypoglycemic coma in the cerebral cortex using diabetic animals, in terms of clinical relevance to hypoglycemia in patients with diabetes.

In the present study, we demonstrated that hypoglycemic coma, even though it is a transient incident, could cause neuronal death and inflammatory response including high expression level of TNFα and microglial activation in a few hours after hypoglycemic coma. In addition, we found characteristic findings for inflammatory response to hypoglycemic brain damage in the cerebral neocortex; 1) large rod-shaped microglia are observed at 3–6 h post-hypoglycemic coma in the neocortical areas where following neuronal degeneration and death are frequently seen; 2) High expression of TNFα could occur transiently 3 h after hypoglycemic coma, even in the cortical area without following neuronal damage. The cortical areas with neuronal degeneration and death exhibit high expression of TNFα that persists up to 6 h after hypoglycemic coma. Our findings suggest that anti-inflammatory treatment for prevention of brain damage in patients with

hypoglycemic coma might be effective when it is performed immediately (within a few hours) after recovery of blood glucose in hypoglycemic coma.

FIGURES AND FIGURE LEGENDS

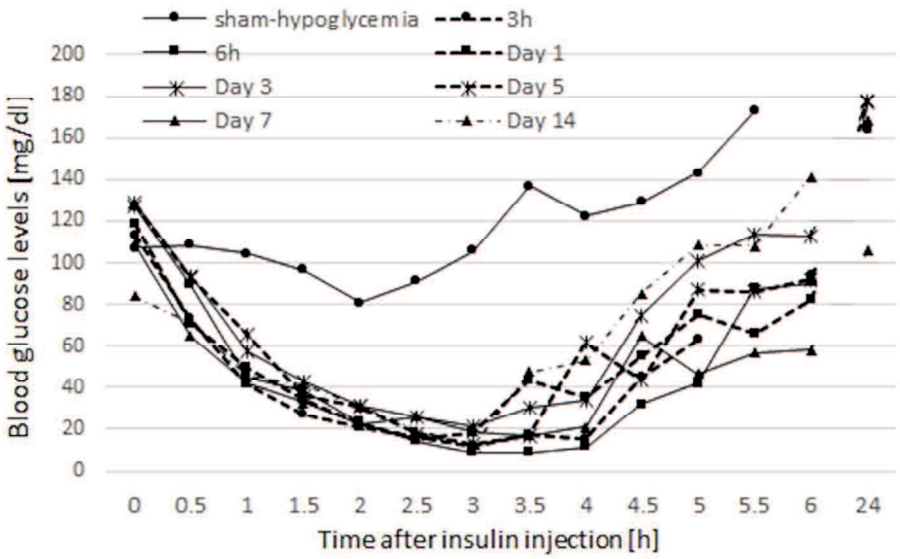

Fig. 1. Blood glucose levels of rats during induced hypoglycemia or sham-hypoglycemia. The blood glucose levels dropped below 20 mg/dl within 2.5–3.5 h after administration of insulin injection in all groups of hypoglycemic rats. All rats quickly recovered consciousness after administration of glucose injection. The blood glucose reached the pre-insulin injection levels within 6 h after administration of insulin injection. Rats with sham-hypoglycemia exhibited minimal decrease of the blood glucose only and the blood glucose levels were maintained above 60 mg/dl.

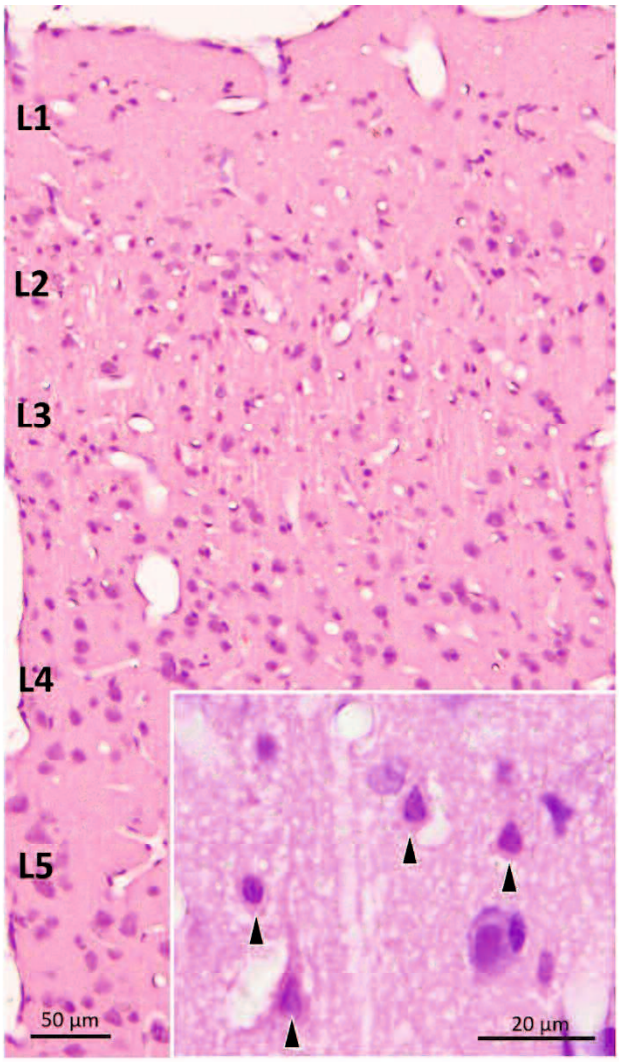

Fig. 2. The cerebral neocortex at 1 day after hypoglycemia. Neurons with acidophilic and shrunken cytoplasm and pyknotic nuclei are diffuse in lamina 2 and 3 (arrowheads). Neuropils of lamina 2 and 3 and the periphery of the acidophilic neurons are edematous. L1-5: lamina 1-5. HE stain.

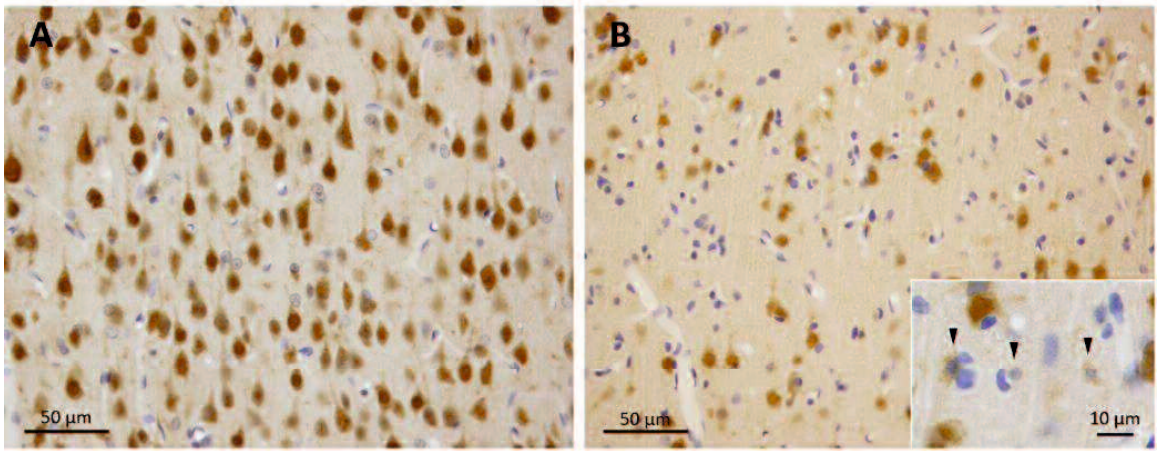

Fig. 3. Immunohistochemistry for neuronal nuclei (NeuN) in the cerebral neocortex lamina 2 and 3 of the control (A) and at 1 day after hypoglycemia (B). A: Neurons exhibiting NeuN-positive nuclei and cytoplasm are densely present. B: NeuN-positive neurons are scattered and the positive signals weaker than those of control animals. B (Inset): Neurons with acidophilic and shrunken cytoplasm and pyknotic nuclei in HE staining exhibit negative to minimally positive NeuN immunoreactivity in the cytoplasm and NeuN negativity in the nuclei.

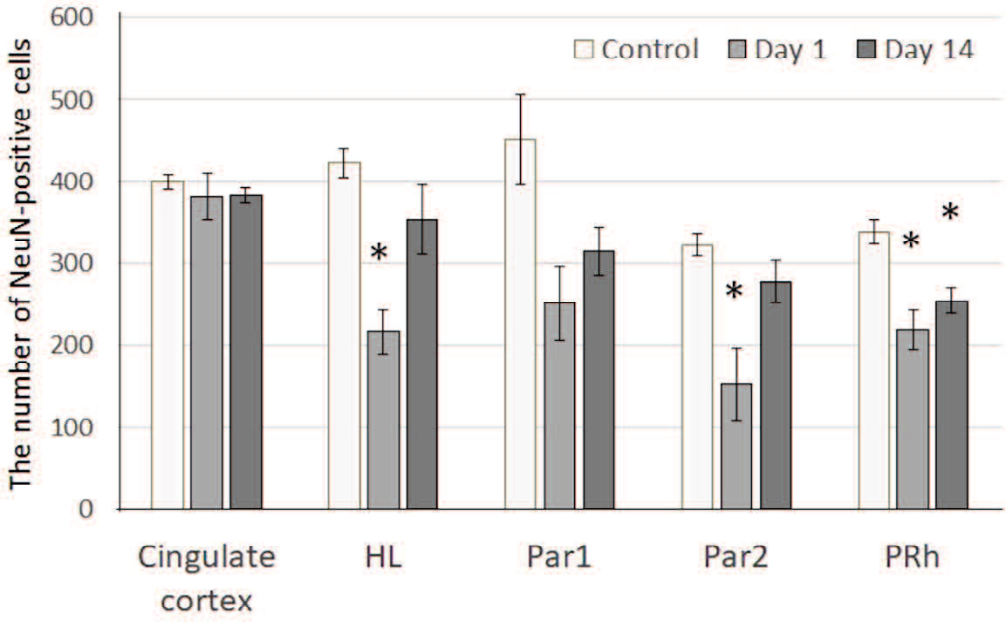

Fig. 4. The number of NeuN-positive cells in lamina 2–3 of the cingulated cortex (n= 3) and four areas of the cerebral neocortex (day1, n=3; day14, n=5). HL: hindlimb area, Par1: parietal cortex area 1, Par2: parietal cortex area 2, PRh: perirhinal cortex. The number of NeuN-positive cells decreased significantly in the HL, Par2 and PRh areas of the neocortex 1 day after hypoglycemia. A significant decrease in the number of NeuN-positive cells was observed only in the PRh 14 days after hypoglycemia. A significant decrease in the number of NeuN-positive cells was not observed in the cingulate cortex.

* $P < 0.05$.

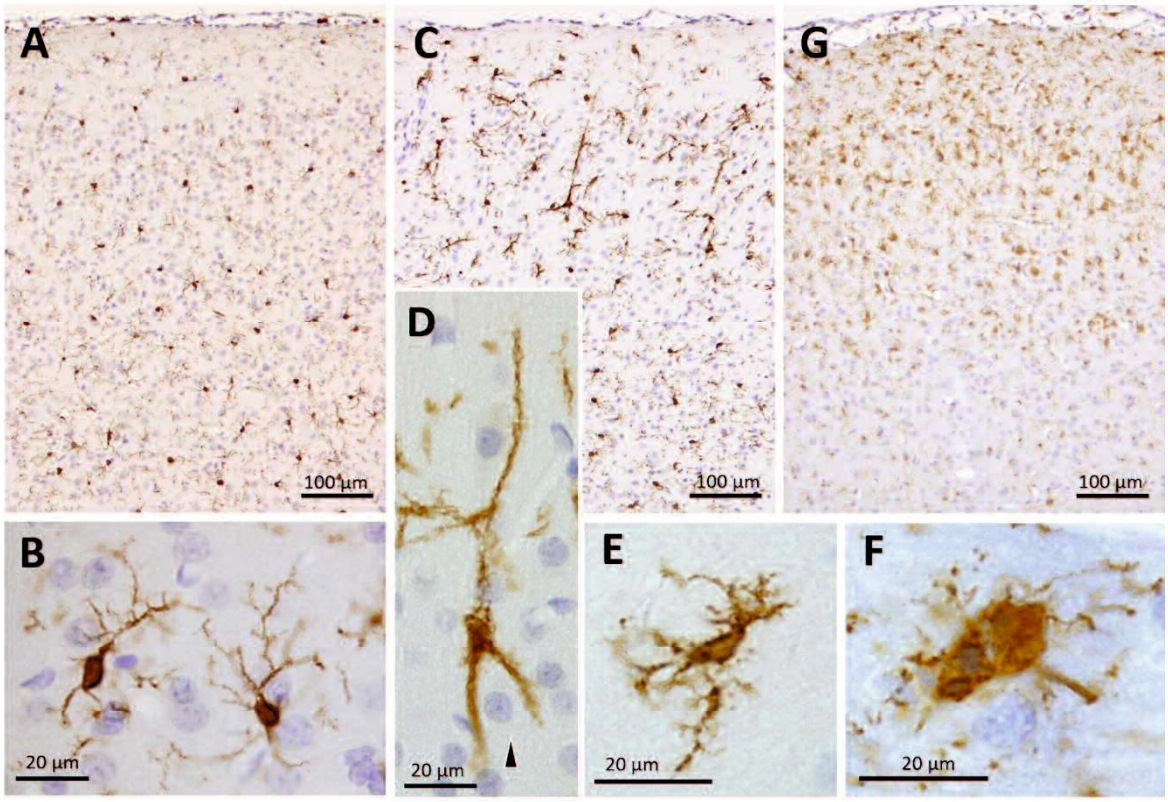

Fig. 5. Immunohistochemistry for Iba-1 in the cerebral neocortex of control (A, B), at 6 h (C, D) and 5 days (E, F, G) after hypoglycemia. A, B: In control animals, most of the Iba-1-positive microglia are spread evenly and exhibit a ramified shape with fine and highly branched dendrites. C, D: At 6 h after hypoglycemia, rod-shaped microglia are observed in lamina 2 and 3. They have long (maximum 200 μm) and straight dendrites that often run perpendicular to the brain surface. Rod-shaped microglia occasionally appear to have contact with neurons (D, arrowhead). E: Hypertrophic microglia have shorter and thicker dendrites. F: Ameboid-shaped microglia exhibit no dendrites or

retracted dendrites and round- to irregularly-shaped cell bodies. G: Iba-1-positive microglia infiltrate lamina 1 to 3; most exhibit a hypertrophic or ameboid shape.

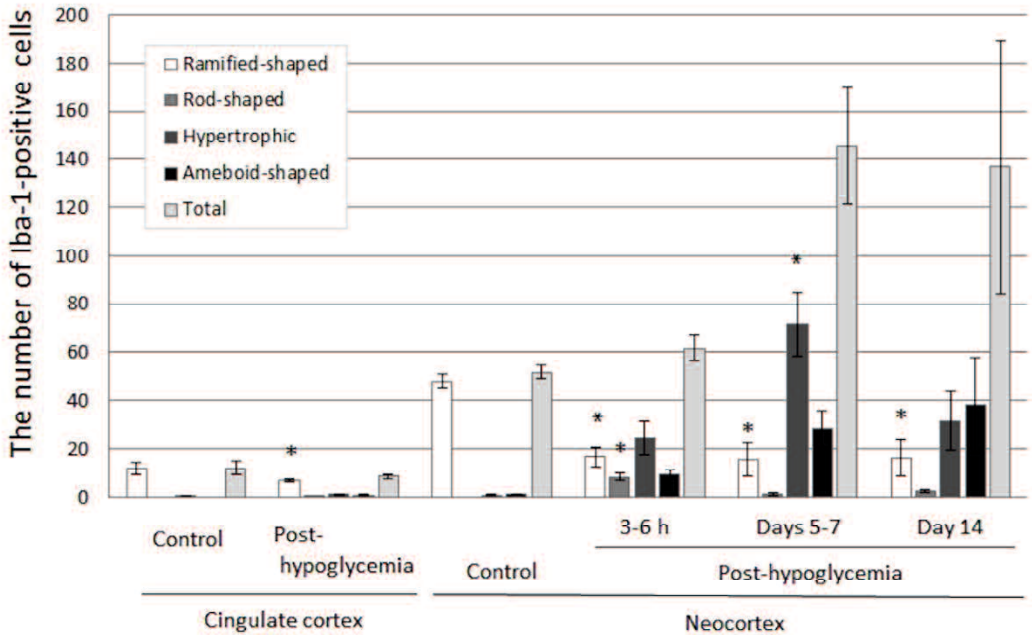

Fig. 6. The number of Iba-1-positive cells in lamina 2 and 3 of the cingulated cortex and cerebral neocortex (control, n= 3; 3–6 h, n= 6; days 5–7, n= 4; day 14, n=4). The cingulate cortex: mild decrease of the number of ramified-shaped microglia is observed. The cerebral neocortex: At 3-6 h, the number of rod-shaped microglia increased. At days 5-7 after hypoglycemia, the number of hypertrophic microglia and ameboid microglia increased. The number of ramified-shaped cells decreased and rod-shaped microglia were rarely observed in the neocortex at days 5-7 post-hypoglycemia. The number of hypertrophic and ameboid-shaped cells tended to increase at day 14 compared to the controls. The number of ramified cells also decreased at day 14 post-hypoglycemia. * $P < 0.05$.

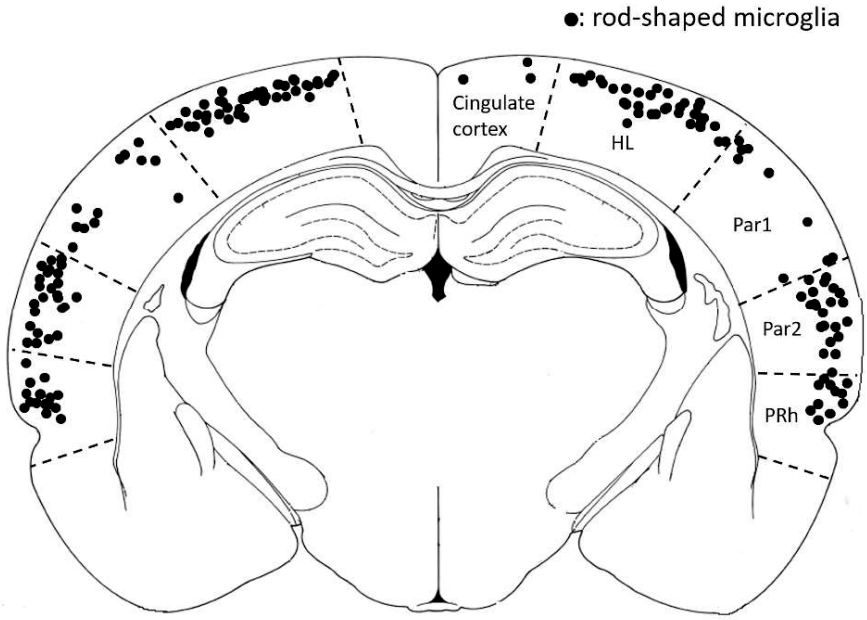

Fig. 7. Schematic diagram of the cerebral hemispheres for assessment of distribution of rod-shaped microglia. Rod-shaped microglia are often recognized in the surface layers of the HL, Par2 and PRh areas and rarely seen in the deeper layers of the neocortex or cingulate cortex. The Par1 area exhibited relatively sparse distribution compared to other areas of the neocortex.

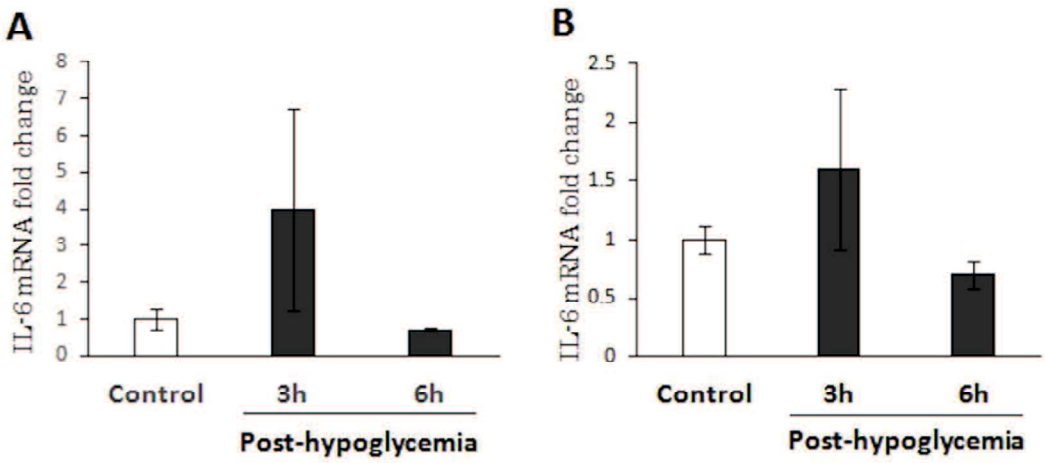

Fig 8. Levels of TNF α mRNA in the cingulate cortex (A) and cerebral neocortex (B) at 3 and 6 h post-hypoglycemia (n= 4 per group). A: In the cingulate gyrus, the mRNA levels of TNF α siginifiantly increased only at 3 h post-hypoglycemia. B: In the neocortex, the mRNA levels of TNF α significantly increased at 3 and 6 h post-hypoglycemia. ** P <0.01.

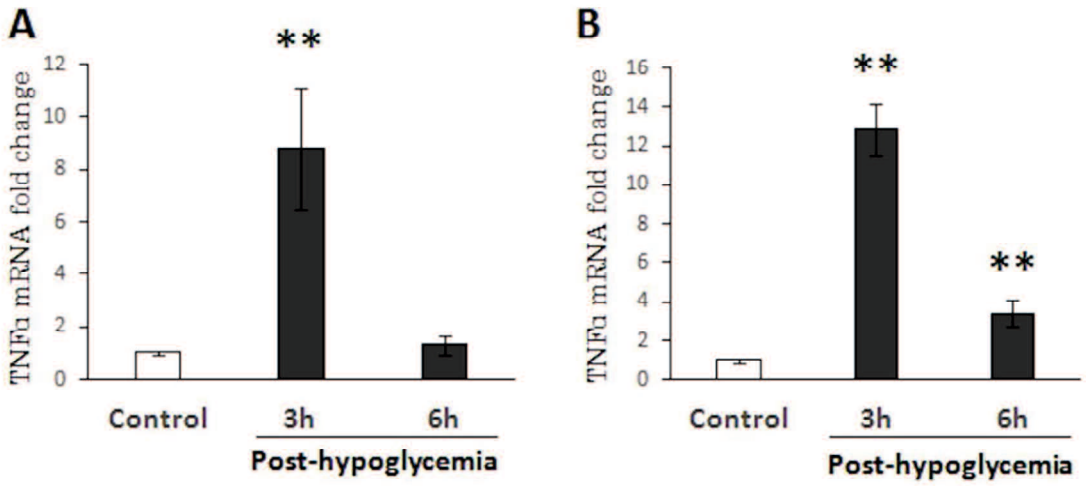

Fig. 9. Levels of IL-6 mRNA in the cingulate cortex (A) and cerebral neocortex (B) at 3 and 6 h post-hypoglycemia (n= 4 per group). A, B: the mRNA levels of Il-6 exhibit no significant change in the cingulate cortex or cerebral neocortex at any time.

CHAPTER 2

Histopathological and immunohistochemical anlyses

of the cerebral white matter

after insulin-induced hypoglycemic coma

ABSTRACT

Patients with hypoglycemic coma exhibit abnormal signals in the white matter on magnetic resonance imaging. Further, the distribution of the abnormal signals had association with the patients' short-term outcomes. However, precise pathological changes in the white matter caused by hypoglycemia remain unclear in humans and experimental animals. We aimed to reveal the distribution and time course of histopathological and immunohistochemical changes occurring in the white matte during the early stages of transient experimental hypoglycemic coma. Insulin-induced hypoglycemic coma of 15–30 min duration was induced in rats, following which the rats were recovered using a glucose solution. Rat brains were collected after 6 and 24 h, and after 3, 5, 7, and 14 days post-hypoglycemic coma. The brains were submitted for histological analysis using hematoxylin and eosin staining, Klüver-Barrera staining, Bodian's staining, and for immunohistochemical analysis using primary antibodies for neurofilament 200 kDa (NF), myelin basic protein, oligodendrocyte transcription factor, ionized calcium-binding adaptor molecule 1 (Iba-1) and glial fibrillary acidic protein (GFAP) analyses. Histologically, vacuolation was observed in the fiber bundles of the globus pallidus from the brains obtained days 1–14. Most of the vacuoles were located in GFAP-positive astrocytic processes or in the extracellular space and appeared to be

edematous. Additionally, myelin pallor and a decrease in NF-positive signals were observed on day 14. Microglial infiltration to the fiber bundles and astrogliosis were also detected. Observations similar to the globus pallidus, except for edema, were also noted in the internal capsule. In the corpus callosum, a mild decrease in NF-positive signals, microgliosis, and astrogliosis were observed. These results suggest that after transient hypoglycemic coma, edema and/or degeneration occurred in the white matter, especially in the globus pallidus, internal capsule, and corpus callosum in the early stages.

INTRODUCTION

Severe hypoglycemia causes gray matter damage that is characterized by neuronal necrosis in the Cornu Ammonis 1 (CA1) of the hippocampus, dentate gyrus, subiculum, cerebral cortex, caudate, and putamen in experimental animals and humans (Auer et al., 1984a; Auer et al., 1989). In contrast, few reports have demonstrated pathological changes in the white matter, in response to severe hypoglycemia. Recent reports have demonstrated that in patients with severe hypoglycemia, hyperintensities were observed by diffusion-weighted magnetic resonance imaging (DWI) in the white matter such as the internal capsule, splenium of corpus callosum, globus pallidus, and/or centrum semiovale. Further, the distribution of abnormal signals had association with the patients' short-term outcomes (Ma et at., 2009; Hegde et al., 2011; Johkura et al., 2012). However, to our knowledge, no reports have demonstrated histopathological and immunohistochemical findings in the white matter, including, axon, myelin, and oligodendrocytes, following exposure to severe hypoglycemia in rat brain. Some reports of human cases of hypoglycemia showed histological observations in the white matter, but they were often reported in severe and chronic cases, where it is difficult to detect primary changes (Auer et al., 1989; Mori et al, 2006).

Therefore, there is a need of defining the histological and immunohistochemical characteristics of the white matter that are produced in response to transient severe hypoglycemia, using animal models. We aimed to reveal the distribution and progression of histological and immunohistochemical findings in the white matter (axons, myelin, and glial cells)

MATERIALS AND METHODS

Animals' procurement and Hypoglycemic treatment

Male Sprague-Dawley rats (210-310 g) were given insulin-induced hypoglycemic coma and recovery using glucose as described above. Control animals were given sham-hypoglycemic treatment as described above.

Tissue preparation for histology and immunohistochemistry

Rats were killed after 6 and 24 h, and on days 3, 5, 7, and 14 post-hypoglycemic coma (n= 2–7 per group). Animals were deeply anesthetized and as intra-aortically perfused with saline and 10% neutral phosphate-buffered formalin as described above. Soon after perfusion, the brains were removed and sectioned coronally into 2-mm thick slices; two of the sections (Bregma -1.8 mm and -3.8 mm) were made into paraffin blocks as mentioned above for histological and immunohistochemical analyses. Four-μm thick paraffin sections were cut from each tissue block for HE staining, Klüver-Barrera (KB) staining, Bodian's staining, and immunohistochemistry.

Immunohistochemical procedure

Immunohistochemical analysis was performed as mentioned above using a mouse monoclonal anti- human glial fibrillary acidic protein (GFAP) antibody (diluted 1:400, Dako Denmark, Glostrup, Denmark), a rabbit polyclonal anti- ionized calcium-binding adaptor molecular 1 (Iba-1) antibody (diluted 1:2000, Wako, Osaka, Japan), a mouse monoclonal anti-myelin basic protein (MBP) antibody (diluted 1:1000, Merk, Darmstadt, Germany), a mouse monoclonal anti-neurofilament antibody (diluted 1:500, Millipore, Massachusetts, USA), or a rabbit polyclonal anti-oligodendrocyte transcription factor (olig-2) antibody (diluted 1:500, Millipore) at 4° C overnight.

Scoring of histopathological and immunohistochemical alterations

We used histopathological and immunohistochemical parameters listed in Table 1 to objectively assess the degree of neuronal necrosis and white matter degeneration. Assessment of neuronal necrosis was performed in the neocortex, hippocampal dentate gyrus, CA1 of hippocampus, and caudoputamen. The assessment of white matter degeneration was performed in the globus pallidus, internal capsule, and corpus callosum. Each brain region was scored from 0 to 3 for each parameter, with the higher score indicating the more significant pathological condition. Six parameters of white matter degeneration were evaluated and the total score was obtained for each white matter region

in each animal. Furthermore, the average scores of all animals that were killed at a particular point of time were obtained for each brain region.

Statistical analysis

Pearson's correlation coefficient was used to investigate correlation between the score of neuronal necrosis and total score of white matter degeneration (the neocortex, hippocampal dentate gyrus, CA1 of hippocampus, or caudoputamen vs the globus pallidus, internal capsule or corpus callosum) at each time-point. The test of significance for correlation coefficients was performed using two-sample, two tailed Student's t-test. P-values < 0.05 were considered statistically significant.

Parameters	Score	Degree of pathological findings
Neuronal necrosis	0	None
	1	Occasionally
	2	Often
	3	Mostly
Variously sized vacuoles in the white matter (Vacuolation)	0	None
	1	Occasionally
	2	Often
	3	Densely
Decrease of NF-positive signals	0	Undetectable. Densely arranged axons with distinct positive signals
	1	Mild. Decreased density of axons with weak positive signals
	2	Moderate. Scattered axons with weaker and indistinct positive signals
	3	Marked. Rare positive signlas
Decrease of MBP-positive signals	0	Undetectable. Homogenous positive signals in a fiber bundle
	1	Mild. Inhomogenous positive signals in a fiber bundle
	2	Moderate. Negative signals in most part of each fiber bundle
	3	Marked. Rare positive signals
Decrease of olig-2-positive signals	0	Undetectable
	1	Mild. Diffusely weak positive signals
	2	Moderate. Scattered positive signals
	3	Marked. Rare positive signals
Increase of Iba-1-positive microglia (Microgliosis)	0	Undetectable
	1	Mild increase with activated morphology
	2	Moderate increase with activated morphology and occasional microglial nodules
	3	Marked increase with activated morphology and many microglial nodules
Increase of GFAP-positive astrocytes (Astrogliosis)	0	Undetectable
	1	Mild increase with slightly thickened dendrites
	2	Moderate increase with thickened dendrites
	3	Marked increase with hypertrophic morphology

Table 1. Protocol of histopathological and immunohistochemical scoring system

NF, neurofilament 200 kDa; MBP, myelin basic protein;
olig-2, oligodendrocyte transcription factor; Iba-1, ionized calcium-binding adaptor molecule 1;
GFAP, glial fibrillary acidic protein.

RESULTS

Histopathology

In the globus pallidus, one case showed spheroid-like changes in the fiber bundles 14 days after hypoglycemic coma (Fig. 1A). Vacuolation of the fiber bundles was observed in the globus pallidus from days 1 to 14 after hypoglycemic coma via KB staining, while neuronal necrosis was rarely noted in the gray matter of the globus pallidus (Fig. 2). One case on day 3 showed myelin debris in the fiber bundles of the globus pallidus that suggested myelin disruption. Myelin pallor was observed in the globus pallidus 14 days after hypoglycemia (Fig. 3). No significant changes in Bodian's staining were detected in any of the brain regions assessed.

Neuronal necrosis was observed in the neocortex, hippocampal dentate gyrus, hippocampal CA1 region, and caudoputamen (Table 2). There was diffuse neuronal necrosis in lamina 2 and 3 of the neocortex as early as 6 h and up to 14 days after hypoglycemic coma. Neuronal necrosis was observed in the dentate gyrus 6 h and persisted up to 14 days after hypoglycemic coma, with the most severe cases appearing from 24 h to 5 days after hypoglycemic coma. The crest of the dentate gyrus was the most commonly affected region exhibiting dense neuronal necrosis. In CA1 of the

hippocampus, neuronal necrosis appeared 3 days after hypoglycemic coma and persisted up to 14 days after hypoglycemic coma. The most severe neuronal necrosis in the CA1 area was observed 3–5 days after hypoglycemic coma. The caudoputamen exhibited neuronal necrosis as early as 6 h and up to 14 days after hypoglycemic coma, especially in lateral areas adjacent to the external capsule. The most severe neuronal necrosis in the caudoputamen was observed 3–7 days after hypoglycemic coma.

Immunohistochemistry

NF-positive signals: NF-positive signals in the fiber bundles of the globus pallidus decreased 14 days after hypoglycemic coma. The number of NF-positive axons decreased and the remaining axons exhibited irregularly flattened shapes in cross sections (Fig. 4). The spheroid-like changes in the globus pallidus were associated with NF-positive signals in one case, 14 days after hypoglycemic coma (Fig. 1B). A decrease in NF-positive signals was also observed in the internal capsule 7 and 14 days after hypoglycemic coma. A mild decrease in NF-positive signals was noted in the corpus callosum on days 3, 5, 7, and 14.

MBP-positive signals: In the fiber bundles of the globus pallidus, a decrease of MBP-positive signals was not detected at 6 hr to 7 days; but was first observed 14 days post-hypoglycemic coma (Fig. 5). This pathology was detected irrespective of the presence of

vacuolation in the fiber bundles of the globus pallidus. The vacuoles in the globus pallidus were occasionally delineated with MBP-positive signals (extracellular edema). The internal capsule exhibited a mild decrease of MBP-positive signals, 7 and 14 days after hypoglycemic coma.

Olig-2-positive signals: There was a decrease in the number of olig-2-positive signals in the globus pallidus 5 and 14 days after hypoglycemic coma (Fig. 6).

Iba-1-positive signals: There was an increase in the number of Iba-1-positive microglial cells in the globus pallidus, 6 h to 14 days after hypoglycemic coma, with the greatest increase occurring between 3 and 14 days. At 6 h post-hypoglycemic coma, the number of microglial cells increased in the globus pallidus with mildly thickened dendrites. On 1, 3, 5, 7, and 14 days post-hypoglycemic coma, microglial cells focally infiltrated into the fiber bundles of the globus pallidus (Fig. 7A, B). Some of the microglial cells exhibited an ameboid shape with short and thickened dendrites. While, some cases showed microgliosis without vacuolation, fiber bundle vacuolation was always accompanied by microglial infiltration. The number of Iba-1-positive cells increased in the internal capsule from 6 hr to 14 days after hypoglycemic coma and their highest infiltration was observed 14 days after hypoglycemic coma. Iba-1-positive microglial cells densely infiltrated from the external toward the ventral side of the internal capsule (Fig.

7C, D). In the corpus callosum, a mild increase in the number of Iba-1-positive microglial cells was observed in most cases from 6 h to 5 days after hypoglycemic coma and in two cases on 14 days. Microglial cells occasionally appeared rod-shaped and were situated along the neuronal fibers in the corpus callosum (Fig. 7E, F).

GFAP-positive signals: In the globus pallidus, the number of GFAP-positive astrocytes was increased on 1 day and up to 14 days after hypoglycemic coma. In fiber bundles of the globus pallidus, GFAP-positive astrocytes often contained vacuoles in their processes (intracellular edema) (Fig. 8). In the ventral region of the internal capsule, a mild increase in the number of GFAP-positive astrocytes was observed, 5–14 days post-hypoglycemic coma. A moderate activation of astrocytes in the corpus callosum was noted in a few cases on 3 and 14 days after hypoglycemic coma, and the activated GFAP-positive astrocytes exhibited slightly elongated dendrites.

Correlation between scores of gray matter regions and those of white matter regions

There was no significant correlation between the score of neuronal necrosis and total score of white matter degeneration in any combinations at any time-points (The date is not shown). In addition, two cases exhibited decrease in the NF, MBP, and olig-2 related

immuno-reactivity and myelin pallor in the globus pallidus on 14 days after hypoglycemic coma, while the neuronal necrosis was not detected in the hippocampal CA1 and caudoputamen.

DISCUSSION

In this study, we revealed degeneration of axons, myelin, and/or oligodendrocytes in the globus pallidus, internal capsule and corpus callosum after transient hypoglycemic coma. The Wallerian degeneration of axons with neuronal cytolysis occurs in the rat dentate gyrus and hippocampal CA1 after hypoglycemia (Auer et al., 1984a; Pramming et al., 1991). However, to our knowledge, no reports have demonstrated histopathological and immunohistochemical characteristics in the white matter, including axons, myelin, and oligodendrocytes, after experimental hypoglycemic coma in the rat cerebrum. Therefore, this is the first report to demonstrate histopathological and immunohistochemical changes in axons, myelin, and oligodendrocytes with reaction of microglia and astrocytes in response to experimental hypoglycemic coma.

We also observed neuronal necrosis in CA1 of the hippocampus, subiculum, dentate gyrus, lamina 2 and 3 of the neocortex as well as caudoputamen that preceded the white matter degeneration. The distribution of neuronal necrosis was consistent with previous studies in hypoglycemic brain damage (Auer et al., 1985; Dommergues et al., 2003; Cordonnier et al.,2005; Deng et al., 2014). Of the brain regions showing neuronal necrosis after hypoglycemic coma, the caudoputamen have efferent projections to the globus

pallidus, and the cerebral cortex has efferent projections to the internal capsule and corpus callosum (Leonard et al., 1969; Preston et al., 1980; Haring et al., 1986; Kincaid et al., 1991; Molyneaux et al., 2007). Therefore, it might be possible that the degeneration of axons and myelin in the globus pallidus, internal capsule, and corpus callosum occurred secondarily to neuronal necrosis in the caudoputamen or cerebral cortex. However, we could not find significant correlations between neuronal necrosis in the gray matter and pathological changes in the white matter. In addition, we found some cases in which white matter degeneration and microgliosis were present in the globus pallidus, without the occurrence of neuronal necrosis in the caudoputamen, 14 days after hypoglycemic coma. These results suggest that axonal degeneration can occur primarily after transient hypoglycemic coma independent of neuronal necrosis in the caudoputamen. Excitotoxicity is one of the most important factors in the pathogenesis of neuronal necrosis after severe hypoglycemia (Auer et al., 2004; Languren et al., 2013). The excitotoxic process is initiated by the release of excitatory amino acids, especially aspartate, in response to glucose deprivation that triggers the excess influx of Ca^{2+} into cells and results in oxidative stress (Norberg et al., 1976; Sandberg et al., 1986; Patočková et al., 2003). Recent studies have demonstrated that excitotoxicity may also cause damage to the white matter (Matute et al., 2007; Lima et al., 2008；Yanget al., 2014). In addition,

a prior report demonstrated the microglial activation within 24 h after excitotoxic brain damage in a neonatal mouse model (Dommergues et al., 2003). In our study, early activation of microglia was observed in the white matter at 6 h after hypoglycemic coma, preceding the degeneration of myelin and the decrease of NF and olig-2-immunoreactivity. These findings suggest that excitotoxic processes could have contributed to the primary white matter damage.

We noted astrocytic-intracellular and extracellular edema in the globus pallidus 1–14 days post-hypoglycemic coma. Disruption of the blood brain barrier (BBB) is one of causes for edema after hypoglycemia (Gisselsson et al., 1998; Deng et al., 2014). One previous report showed that disruption of the BBB caused by hypoglycemia occurred after 24 h of recovery and contributed to edema formation (Deng et al., 2014). Moreover, it takes many weeks to clear excess waters, proteins, and ions from brain tissue (Thrane et al., 2014). In our study, edema in the globus pallidus was observed 1–14 days after hypoglycemic coma, which suggests that disruption of the BBB might contribute to the edema in the globus pallidus.

In contrast, edema was not detected in the internal capsule and the corpus callosum. Edema can also occur immediately after hypoglycemic coma before the recovery, when the BBB has not yet been disrupted (Kalimo et al., 1985; Gisselsson et al., 1998; Deng et

al., 2014). Such edema in the early phase seems to result from an increase oin intracellular Na^+ because of the dysfunction of energy-dependent ion transporters (Deng et al., 2014). Recent studies have demonstrated acute changes in patients with hypoglycemic coma, which were detected using diffusion-weighted MRI (DWI). The observations using DWI are valuable for detecting acute and primary brain damage in patients with severe hypoglycemia. DWI of hypoglycemic patients revealed hyperintensities and reduced apparent diffusion coefficients in white matter, including the internal capsule and corpus callosum; the abnormal DWI signals in white matter were often observed during comatose hypoglycemia and disappeared immediately after recovery of consciousness by glucose injection (Aoki et al., 2004; Cordonnier et al., 2005; Maekawa et al., 2006; Ma et al., 2009; Hegde et al., 2011; Johkura et al. 2012). Abnormal DWI signals observed in hypoglycemia were considered to reflect intracellular edema (Auer et al., 1985; Hasegawa et al., 1996; Schaefer et al., 2000; Maekawa et al., 2006). These reports suggest that edema in the white matter rarely causes the BBB disruption and often disappears immediately after glucose injection in human cases of hypoglycemia. In our study, edema was only recognized in the globus pallidus, but not in the internal capsule and the corpus callosum. It might be possible that the transient edema had in fact occurred; however, the BBB disruption did not occur, and the edema recovered because of glucose injection as

seen in human studies.

In conclusion, we revealed that transient hypoglycemic coma causes white matter damage in the globus pallidus, internal capsule, and corpus callosum, and that the excitotoxic processes might have independently contribute to the primary white matter damage. We also defined the histopathological and immunohistochemical characteristics of white matter damage caused by hypoglycemia, such as extracellular and intracellular edema, axonal degeneration, myelin pallor, and activation of microglia and astrocytes. The prevention and/or treatment of the white matter damage may contribute to development of new strategies for the prevention and/or treatment of hypoglycemic brain damage. However, we need more investigation of the pathogenesis of the white matter damage in response to hypoglycemic coma, including the correlation between the white matter degeneration and edema.

FIGURES AND FIGURE LEGENDS

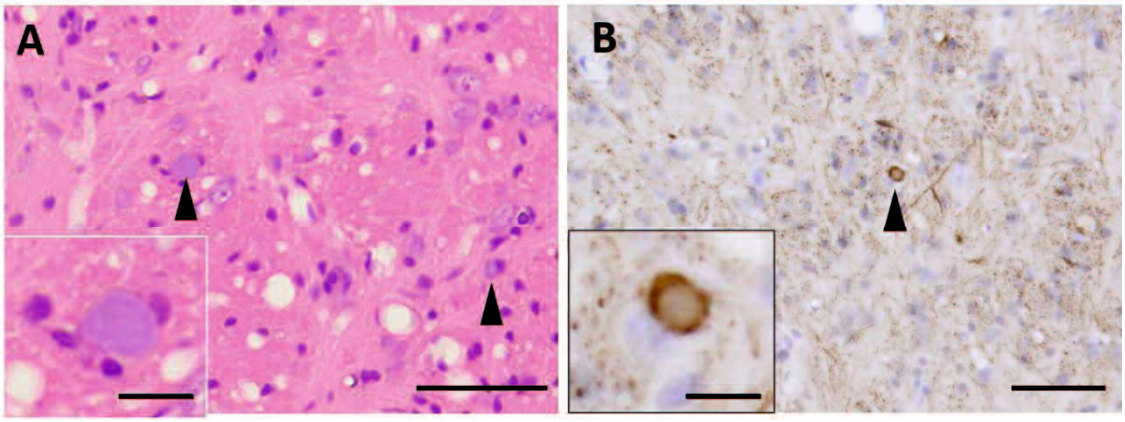

Fig. 1. Histopathological and immunohistochemical figures of the globus pallidus. Hematoxylin and eosin staining (A), immunohistochemistry for neurofilament 200 kDa (NF) (B). (A) 14 days after hypoglycemic coma. Spheroid-like structures were scattered in the fiber bundles (arrowheads). (A, Inset) High magnification of a spheroid-like structure. (B) 14 days after hypoglycemic coma. A NF-positive signal in the spheroid-like structure. (B, Inset) High magnification of a spheroid-like structure exhibiting NF-positive signal. Bar= 50 μm, Insets: Bar= 10 μm.

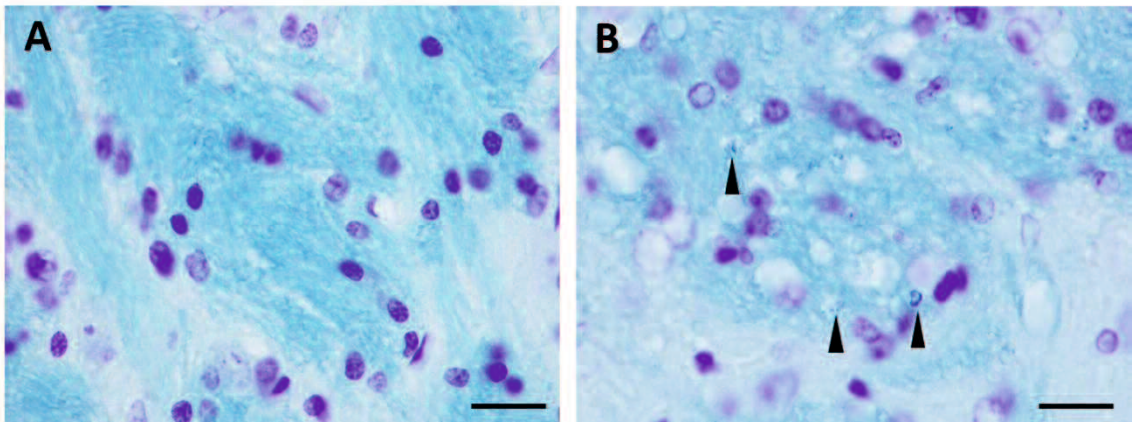

Fig. 2. Histopathological figures of the globus pallidus. Klüver-Barrera staining. (A) Sham-hypoglycemic coma (score 0). (B) 3 days after hypoglycemic coma. Vacuoles were observed in the fiber bundles (score 1). Myelin debris were scattered (arrowheads). Bar= 20 μm.

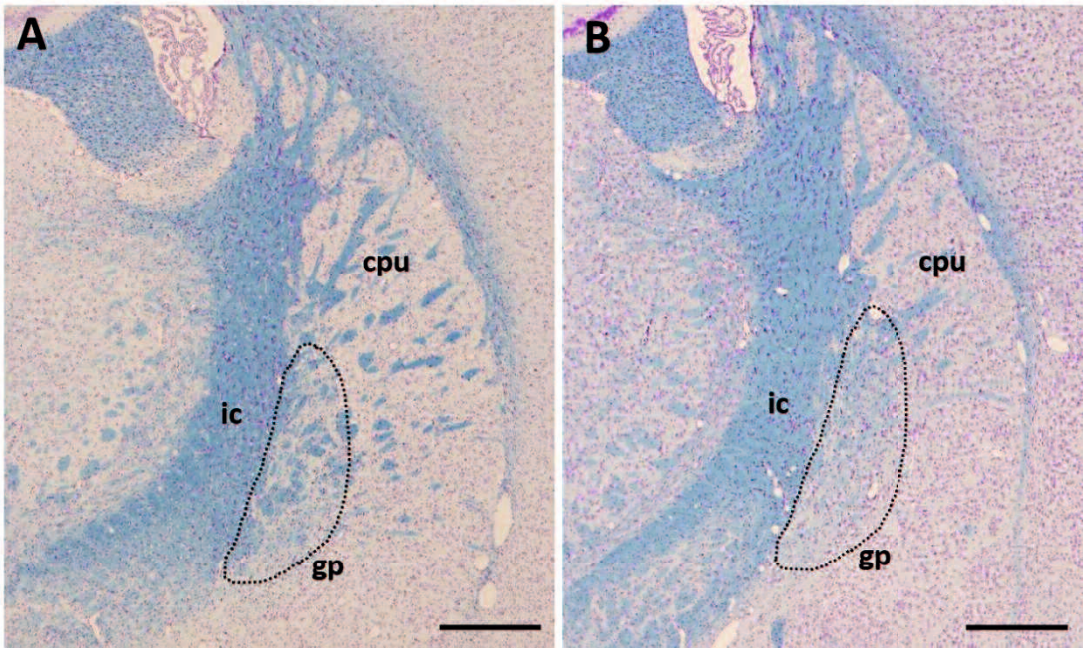

Fig. 3. Histopathological figures of the globus pallidus. Klüver-Barrera staining. (A) Sham-hypoglycemic coma. (B) 14 days after hypoglycemic coma. Myelin pallor in the grobus pallidus (broken line). ic: internal capsule, gp: globus pallidus, cpu: caudoputamen. Bar= 500 μm.

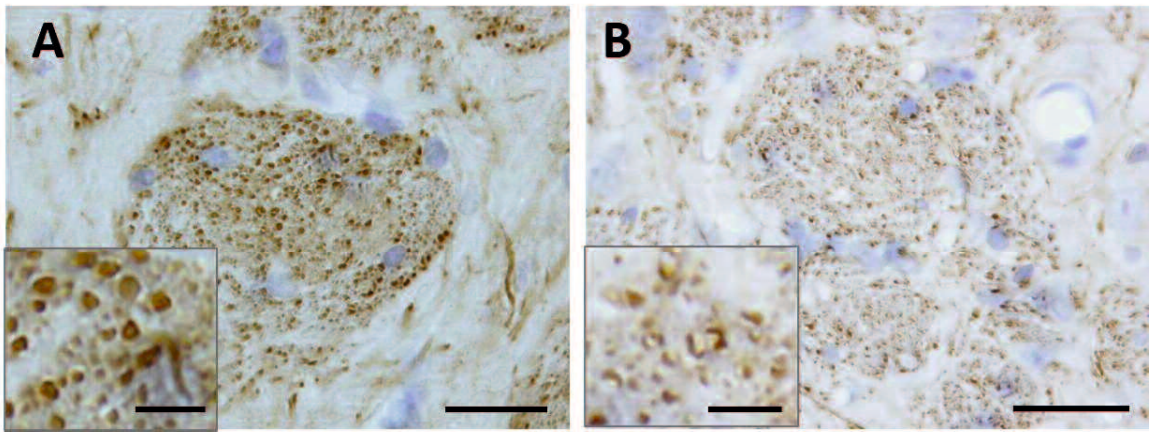

Fig. 4. Immunohistochemical figures of NF in the globus pallidus. (A) Sham-hypoglycemic coma. (A, Inset) High magnification of axons. Uniform cross-sections of NF-positive axons in the fiber bundles (score 0). (B) The globus pallidus 3 days after hypoglycemic coma. A decrease of NF-immunoreactivity in fiber bundles. (B, Inset) High magnification of axons. Cross sections of axons exhibited irregularly flattened shapes (score 1). Bar= 20 μm, Insets: Bar= 5 μm.

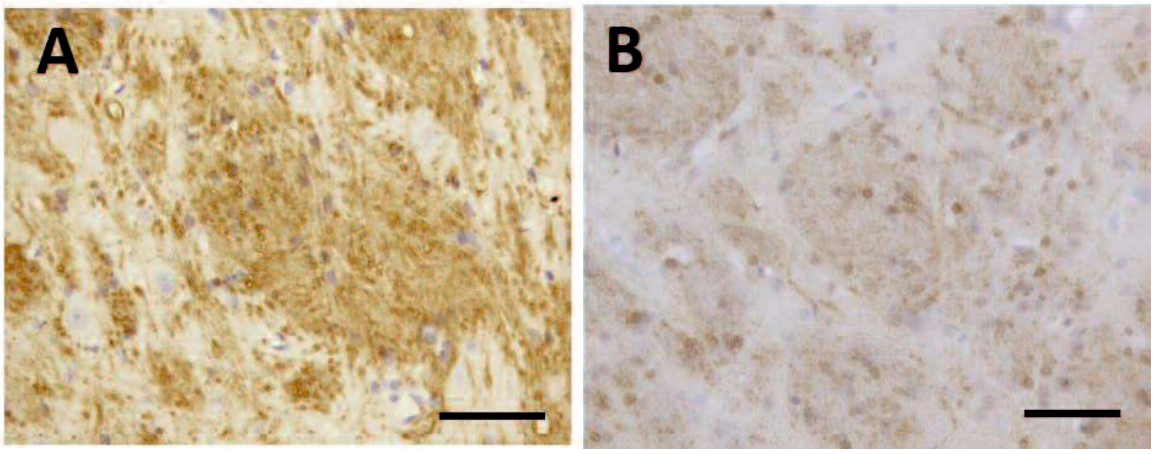

Fig. 5. Immunohistochemical figures of myelin basic protein in the globus pallidus. (A) Sham-hypoglycemic coma. Positive signals were observed in the fiber bundles (score 0). (B) 14 days after hypoglycemic coma. A significant decrease of immunoreactivity in the fiber bundles (score 2). Bar= 50 μ m.

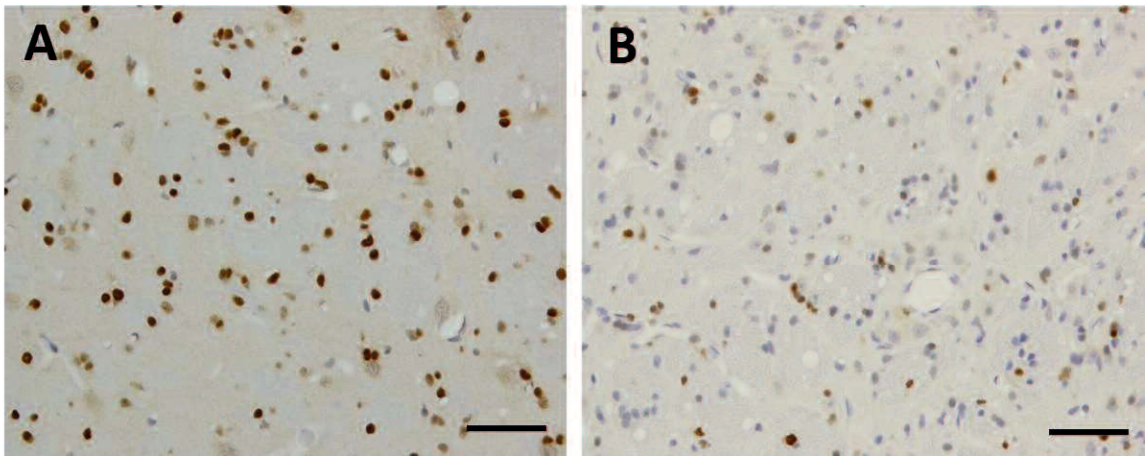

Fig. 6. Immunohistochemical figures of olig-2 in the globus pallidus. (A) Sham-hypoglycemic coma. Strong positive signals in oligodendrocytes (score 0). (B) 14 days after hypoglycemic coma. The number of olig-2 positive signals decreased and each signal was weak compared to that in sham-hypoglycemic control (score 1). Bar= 50 μm.

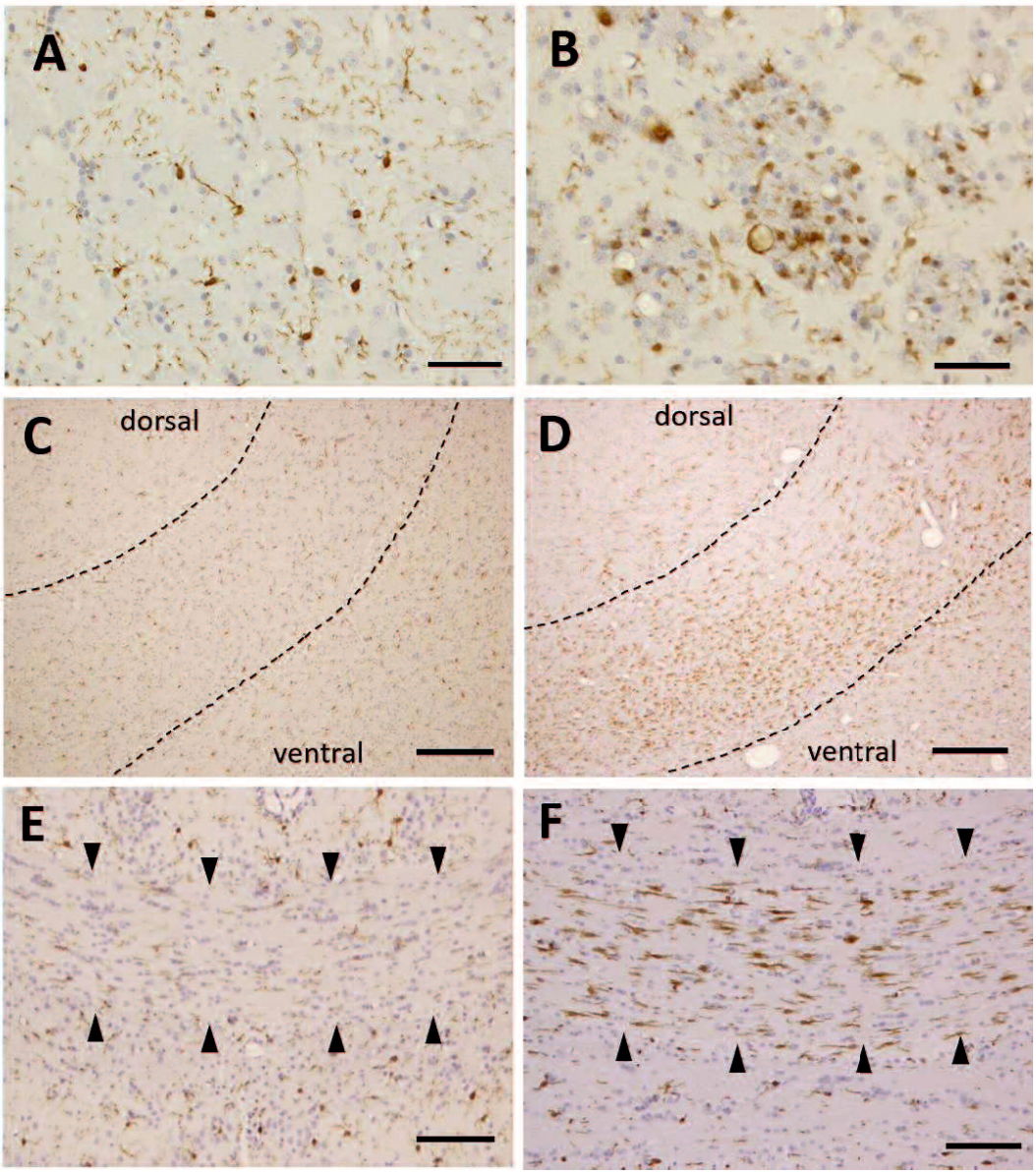

Fig. 7. Immunohistochemical figures of ionized calcium-binding adaptor molecule 1 (Iba-1) in the globus pallidus (A, B), the internal capsule (C, D) and the corpus callosum (E, F). (A) The globus pallidus of sham-hypoglycemic rat. Iba-1-positive microglial cells with thin dendrites were evenly distributed (score 0). (B) The globus pallidus 14 days after hypoglycemic coma. Iba-1-positive microglial cells focally infiltrated into the fiber

bundles. Some microglial cells exhibited an ameboid shape with short and thickened dendrites (score 2). Bar= 20 μm. (C) The internal capsule of sham-hypoglycemic coma (dashed lines) (score 0). (D) The internal capsule 14 days after hypoglycemic coma (dashed lines). Iba-1-positive microglial cells focally infiltrated into the ventral side of the internal capsule (score 2). Bar= 100 μm. (E) The corpus callosum of sham-hypoglycemic rat (arrowheads) (score 0). (F) The corpus callosum 3 days after hypoglycemic coma (arrowheads). The number of Iba-1-positive microglial cells increased and they exhibited thickened rod-shaped dendrites (score 2). Bar= 200 μm.

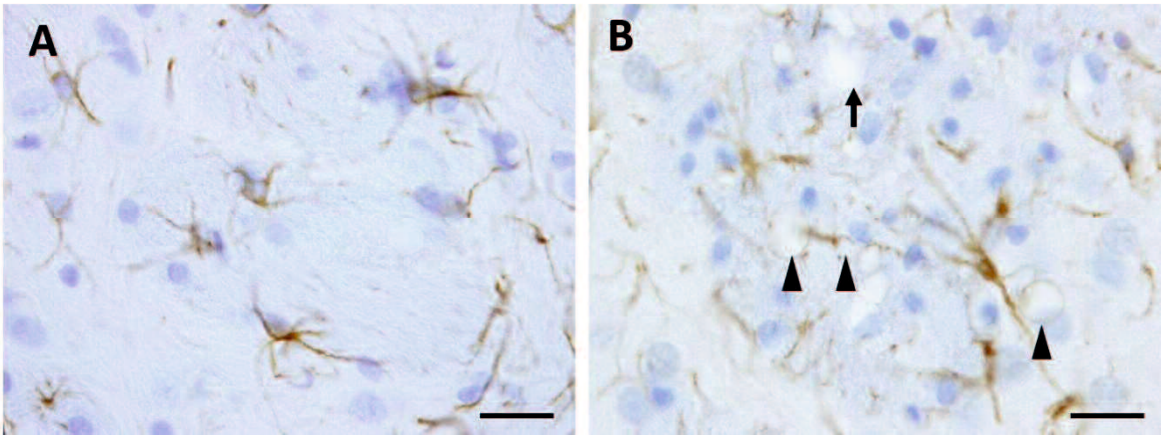

Fig. 8. Immunohistochemical figures of glial fibrillary acidic protein in the globus pallidus. (A) Sham-hypoglycemic coma (score 0). (B) 14 days after hypoglycemic coma. Some vacuoles were present in astrocytic processes (arrowheads). Others were present in extracellular spaces (an arrow) (score 1). Bar= 20 μ m.

White matter			6 hr		24 hr		3 days		5 days		7 days		14 days	
	Globus pallidus		Score	n	Score	n	Score	n	Score	n	Score	n	Score	n
		Variously sized vacuoles in white matter (Vacuolation)	0.0	0 / 2	1.0	1 / 2	0.6	3 / 5	0.5	1 / 4	0.8	2 / 4	0.3	1 / 7
		Decrease of NF-positive signals	0.0	0 / 1	0.0	0 / 1	0.0	0 / 5	0.0	0 / 3	0.0	0 / 2	0.7	3 / 6
		Decrease of MBP-positive signals	0.0	0 / 2	0.0	0 / 2	0.3	1 / 4	0.0	0 / 3	0.0	0 / 3	1.0	4 / 6
		Decrease of olig-2-positive signals	0.0	0 / 2	0.0	0 / 2	0.0	0 / 5	0.3	1 / 3	0.0	0 / 2	0.6	4 / 7
		Increase of Iba-1-positive microglia (Microgliosis)	1.0	2 / 2	0.5	1 / 2	0.8	3 / 5	0.5	1 / 4	1.7	2 / 3	1.7	7 / 7
		Increase of GFAP-positive astrocytes (Astrogliosis)	0.0	0 / 2	0.5	1 / 2	0.4	2 / 5	0.3	1 / 3	0.3	1 / 4	0.5	3 / 6
		Total score	1.0		2.0		2.1		1.6		2.8		4.8	
			6 hr		24 hr		3 days		5 days		7 days		14 days	
	Internal capsule		Score	n	Score	n	Score	n	Score	n	Score	n	Score	n
		Variously sized vacuoles in white matter (Vacuolation)	0.0	0 / 2	0.0	0 / 2	0.0	0 / 5	0.0	0 / 4	0.0	0 / 4	0.0	0 / 7
		Decrease of NF-positive signals	0.0	0 / 1	0.0	0 / 1	0.0	0 / 4	0.0	0 / 3	0.3	1 / 3	0.7	3 / 6
		Decrease of MBP-positive signals	0.0	0 / 1	0.0	0 / 2	0.0	0 / 3	0.0	0 / 3	0.3	1 / 3	0.3	2 / 6
		Decrease of olig-2-positive signals	0.0	0 / 1	0.0	0 / 2	0.0	0 / 2	0.3	1 / 3	0.0	0 / 1	0.0	0 / 7
		Increase of Iba-1-positive microglia (Microgliosis)	0.5	1 / 2	0.5	1 / 2	0.5	2 / 4	0.3	1 / 3	0.3	1 / 4	1.0	5 / 6
		Increase of GFAP-positive astrocytes (Astrogliosis)	0.0	0 / 2	0.0	0 / 2	0.0	0 / 4	0.3	1 / 3	0.3	1 / 3	0.6	3 / 5
		Total score	0.5		0.5		0.5		0.9		1.2		2.6	
			6 hr		24 hr		3 days		5 days		7 days		14 days	
	Corpus callosum		Score	n	Score	n	Score	n	Score	n	Score	n	Score	n
		Variously sized vacuoles in white matter (Vacuolation)	0.0	0 / 2	0.0	0 / 2	0.0	0 / 5	0.0	0 / 4	0.0	0 / 4	0.0	0 / 7
		Decrease of NF-positive signals	0.0	0 / 1	0.0	0 / 1	0.8	3 / 4	0.3	1 / 3	0.5	1 / 2	0.2	1 / 6
		Decrease of MBP-positive signals	0.0	0 / 2	0.0	0 / 2	0.0	0 / 5	0.0	0 / 4	0.0	0 / 4	0.0	0 / 7
		Decrease of olig-2-positive signals	0.0	0 / 1	0.0	0 / 2	0.0	0 / 5	0.3	0 / 3	0.0	0 / 2	0.0	0 / 7
		Increase of Iba-1-positive microglia (Microgliosis)	1.0	2 / 2	0.5	1 / 2	1.2	5 / 5	0.3	1 / 4	0.0	0 / 4	0.3	2 / 7
		Increase of GFAP-positive astrocytes (Astrogliosis)	0.0	0 / 2	0.0	0 / 2	0.2	1 / 5	0.0	0 / 4	0.0	0 / 4	0.1	1 / 7
		Total score	1.0		0.5		2.2		0.9		0.5		0.6	
Gray matter			6 hr		24 hr		3 days		5 days		7 days		14 days	
			Score	n	Score	n	Score	n	Score	n	Score	n	Score	n
	Cerebral neocortex	Neuronal necrosis	0.5	1 / 2	2.0	2 / 2	1.2	5 / 5	1.5	4 / 4	1.0	3 / 4	1.1	7 / 7
	Dentate gyrus	Neuronal necrosis	1.0	2 / 2	1.5	2 / 2	1.2	4 / 5	1.0	2 / 4	0.5	2 / 4	0.7	4 / 7
	CA1 of the hipocampus	Neuronal necrosis	0.0	0 / 2	0.0	0 / 2	0.8	3 / 5	1.3	4 / 4	0.5	2 / 4	0.3	2 / 7
	Caudoputamen	Neuronal necrosis	1.0	2 / 2	1.0	2 / 2	1.6	5 / 5	1.0	3 / 4	1.3	3 / 4	0.7	4 / 7

Table 2. Histopathological and immunohistochemical score and the number of animals exhibiting the finding in each time point after hypoglycemia

Score: an average score of all animals included in the time point
n: the number of animals exhibiting the finding (score 1-3)

CONCLUSIONS

Our results indicate that brains after insulin-induced hypoglycemic coma exhibit not only neuronal death but also various alterations, such as early activation of microglial cell with high expression of TNFα in the cerebral neocortex and myelin and axonal degeneration and edema in the cerebral white matter (the globus pallidus, internal capsule and corpus callosum). Our findings may contribute to the development of new strategies for the prevention and/or treatment of hypoglycemic brain damage.

ACKNOWLEDGEMENTS

The research for this Ph. D. thesis was carried out at Laboratory of Veterinary Pathology, Faculty of Agriculture, Tottori University. I am deeply grateful to my supervisor Professor Dr. Takehito Morita (Laboratory of Veterinary Pathology, Tottori University) for his guidance and his dedication and encouragement during this work. I also thank Associate professor Dr. Yuji Sunden (Laboratory of Veterinary Pathology, Tottori University) for his expert advice and encouragement during whole course of this thesis work. Special thanks to Assistant professor Dr. Masashi Sakurai (Laboratory of Veterinary Pathology, Yamaguchi University) for his heartfelt encouragement. I would like to thank Professor Dr. Masahiro Morimoto (Laboratory of Veterinary Pathology, Yamaguchi University), Professor Dr. Takashi Takeuchi (Laboratory of Veterinary Medicine, Tottori University), and Professor Dr. Yoshiaki Yamano (Laboratory of Veterinary Biochemistry, Tottori University) for their expert advice and encouragement.

REFERENCES

Acarin L, González B, Castellano B. Neuronal, astroglial and microglial cytokine expression after an excitotoxic lesion in the immature rat brain. *Eur J Neurosci* 2000; **12**: 3505–3520.

Aoki T, Sato T, Hasegawa K, Ishizaki R, Saiki M. Reversible hyperintensity lesion on diffusion-weighted MRI in hypoglycemic coma. *Neurology* 2004; **63**: 392–393.

Auer RN. Hypoglycemic brain damage. *Forensic Sci Int* 2004; **146**: 105–110.

Auer RN, Kalimo H, Olsson Y, Wieloch T. The dentate gyrus in hypoglycemia: pathology implicating excitotoxin-mediated neuronal necrosis. *Acta Neuropathol* 1985; **67**: 279–288.

Auer RN. Kalimo H, Olsson Y, Siesjö BK. The temporal evolution of hypoglycemic brain damage. I. Light- and electron-microscopic findings in the rat cerebral cortex. *Acta Neuropathol* 1985; **67**: 13–24.

Auer RN, Hugh J, Cosgrove E, Curry B. Neuropathologic findings in three cases of profound hypoglycemia. *Clin Neuropathol* 1989; **8**: 63–68.

a. Auer RN, Olsson Y, Siesjö BK. Hypoglycemic brain injury in the rat. Correlation of density of brain damage with EEG isoelectric time: a quantitative study. *Diabetes* 1984; **33**: 1090–1098.

b. Auer RN, Wieloch T, Olsson Y, Siesjö BK. The distribution of hypoglycemic brain damage. *Acta Neuropathol* 1984; **64**: 177–191.

Baird TA, Parsons MW, Phan T *et al*. Persistent poststroke hyperglycemia is independently associated with infarct expansion and worse clinical outcome. *Stroke* 2003; **34**: 2208–2214.

Ben-Ami H, Nagachandran P, Mendelson A, Edoute Y. Drug-induced hypoglycemic coma in 102 diabetic patients. *Arch Intern Med* 1999; **159**: 281–284.

Bjorgaas M, Gimse R, Vik T, Sand T. Cognitive function in type 1 diabetic children with and without episodes of severe hypoglycaemia. *Acta Paediatr* 1997; **86**: 148–153.

Bree AJ, Puente EC, Daphna-Iken D,Fisher SJ. Diabetes increases brain damage caused by severe hypoglycemia. *Am J Physiol Endocrinol Metab* 2009; **297**: E194–E201.

Brown GC, Vilalta A. How microglia kill neurons. *Brain Res* 2015; **1628**: 288- 297.

Bruce AJ, Boling W, Kindy MS et al. Altered neuronal and microglial responses to excitotoxic and ischemic brain injury in mice lacking TNF receptors. *Nat Med* 1996; **2**: 788–794.

Cho NH, Shaw JE, Karuranga S et al. IDF Diabetes Atlas: Global estimates of

diabetes prevalence for 2017 and projections for 2045. *Diabetes Res Clin Pract* 2018; **138**: 271–281.

Clayton D, Woo V, Yale J-F. Clinical practice guidelines Hypoglycemia, Canadian diabetes association clinical practice guidelines expert committee. *Can J Diabetes* 2013; **37**: S69–S71.

Cordonnier C, Oppenheim C, Lamy C, Meder J-F, Mas J-L. Serial diffusion and perfusion-weighted MR in transient hypoglycemia. *Neurology* 2005; **65**: 175.

Deng J, Zhao F, Yu X et al. Expression of aquaporin 4 and breakdown of the blood brain barrier after hypoglycemia-induced brain edema in rats. *PLoS ONE* 2014; **9**: e107022.

Dirnagl U, Iadecola C, Moskowitz MA. Pathobiology of ischaemic stroke: an integrated view. *Trends Neurosci* 1999; **22**: 391–397.

Dommergues M-A, Plaisant F, Verney C, Gressens P. Early microglial activation following neonatal excitotoxic brain damage in mice: a potential target for neuroprotection. *Neuroscience* 2003; **121**: 619–628.

Donnelly LA, Morris AD, Frier BM et al. Frequency and predictors of hypoglycaemia in type 1 and insulin-treated type 2 diabetes: a population-based study. *Diabet Med* 2005; **22**: 749–755.

Du Y, Deng W, Wang Z et al. Differential subnetwork of chemokines/cytokines in human, mouse, and rat brain cells after oxygen–glucose deprivation. *J Cereb Blood Flow Metab* 2017; **37**: 1425–1434.

Gisselsson L, Smith M-L, Siesjö BK. Influence of hypoglycemic coma on brain water and osmolality. *Exp Brain Res* 1998; **120**: 461–469.

Graeber MB, Mehraein P. Microglial rod cells. *Neuropathol Appl Neurobiol* 1994; **20**: 178–180.

Graeber MB, Streit WJ. Microglia: biology and pathology. *Acta Neuropathol* 2010; **119**: 89–105.

Hanisch U-K. Microglia as a source and target of cytokines. *Glia* 2002; **40**: 140–155.

Haring JH, Wang RY. The Identification of some sources of afferent input to the rat nucleus basalis magnocellularis by retrograde transport of horseradish peroxidase. *Brain Res* 1986; **366**: 152–158.

Hasegawa Y, Formato JE, Latour LL et al. Severe transient hypoglycemia causes reversible change in the apparent diffusion coefficient of water. *Stroke* 1996; **27**: 1648–1656.

Hegde AN, Mohan S, Lath N, Lim T. Differential diagnosis for bilateral abnormalities of the basal ganglia and thalamus. *RadioGraphics* 2011; **31**: 5–30.

Johkura K, Nakae Y, Kudo Y, Yoshida TN, Kuroiwa Y. Early diffusion MR imaging findings and short-term outcome in comatose patients with hypoglycemia. *AJNR Am J Neuroradiol* 2012; **33**: 904–909.

Kalimo H, Auer RN, Siesjö BK. The temporal evolution of hypoglycemic brain damage. III. Light and electron microscopic findings in the rat caudoputamen. *Acta Neuropathol* 1985; **67**: 37–50.

Kauppinen TM, Higashi Y, Suh SW, Escartin C, Nagasawa K, Swanson RA. Zinc triggers microglial activation. *J Neurosci* 2008; **28**: 5827–5835.

Kettenmann H, Hanisch U-K, Noda M, Verkhratsky A. Physiology of microglia. *Physiol Rev* 2011; **91**: 461-553.

Kincaid AE, Penney Jr. JB, Young AB, Newman SW. The globus pallidus receives a projection from the parafascicular nucleus in the rat. *Brain Res* 1991; **553**: 18–26.

Lambertsen KL, Deierborg T, Gregersen R et al. Differences in origin of reactive microglia in bone marrow chimeric mouse and rat after transient global ischemia. *J Neuropathol Exp Neurol* 2011; **70**: 481–494.

Languren G, Montiel T, Julio-Amilpas A, Massieu L. Neuronal damage and cognitive impairment associated with hypoglycemia: An integrated view. *Neurochem Int*

2013; **63**: 331–343.

Leonard CM. The prefrontal cortex of the rat. I. Cortical projection of the mediodorsal nucleus. II. Efferent connections. *Brain Res* 1969; **12**: 321–343.

Lima RR, Guimaraes-Silva J, Oliveira JL et al. Diffuse axonal damage, myelin impairment, astrocytosis and inflammatory response following microinjections of NMDA into the rat striatum. *Inflammation* 2008; **31**: 24–35.

Lin B, Ginsberg MD, Busto R. Hyperglycemic exacerbation of neuronal damage following forebrain ischemia: microglial, astrocytic and endothelial alterations. *Acta Neuropathol* 1998; **96**: 610-620.

Lo L, Tan CHA, Umapathi T, Lim CC. Diffusion-weighted MR imaging in early diagnosis and prognosis of hypoglycemia. *AJNR Am J Neuroradiol* 2006; **27**: 1222–1224.

Ma J-H, Kim Y-J, Yoo W-J et al. MR imaging of hypoglycemic encephalopathy: lesion distribution and prognosis prediction by diffusion-weighted imaging. *Neuroradiology* 2009; **51**: 641–649.

Maekawa S, Aibiki M, Kikuchi K, Kikuchi S, Umakoshi K. Time related changes in reversible MRI findings after prolonged hypoglycemia. *Clin Neurol Neurosurg* 2006; **108**: 511–513.

Matute C, Alberdi E, Domercq M et al. Excitotoxic damage to white matter. *J Anat* 2007; **210**: 693–702.

McGeer PL, Itagaki S, Boyes BE, McGeer EG. Reactive microglia are positive for HLA-DR in the substantia nigra of Parkinson's and Alzheimer's disease brains. *Neurology* 1988; **38**: 1285–1291.

McPhail LT, McBride CB, McGraw J, Steeves JD, Tetzlaff W. Axotomy abolishes NeuN expression in facial but not rubrospinal neurons. *Exp Neurol* 2004; **185**: 182–190.

Molyneaux BJ, Arlotta P, Menezes JRL, Macklis JD. Neuronal subtype specification in the cerebral cortex. *Nat Rev Neurosci* 2007; **8**: 427–437.

Moreira T, Cebers G, Pickering C, Östenson C-G, Efendic S, Liljequist S. Diabetic Goto-Kakizaki rats display pronounced hyperglycemia and longer-lasting cognitive impairments following ischemia induced by cortical compression. *Neuroscience* 2007; **144**: 1169–1185.

Mori F, Nishie M, Houzen H, Yamaguchi J, Wakabayashi K. Hypoglycemic encephalopathy with extensive lesions in the cerebral white matter. *Neuropathology* 2006; **26**: 147–152.

Murugan M, Ling E-A, Kaur C. Glutamate receptors in microglia. *CNS Neurol*

Disord Drug Targets 2013; **12**: 773–784.

Murugan M, Sivakumar V, Lu J, Ling E-A, Kaur C. Expression of N-Methyl D-Aspartate receptor subunits in amoeboid microglia mediates production of nitric oxide via NF-κB signaling pathway and oligodendrocyte cell death in hypoxic postnatal rats. *Glia* 2011; **59**: 521–539.

Nau R, Brück W. Neuronal injury in bacterial meningitis: mechanisms and implications for therapy. *Trends Neurosci* 2002; **25**: 38–45.

Norberg K, Siesjö BK. Oxidative metabolism of the cerebral cortex of the rat in severe insulin-induced hypoglycemia. *J Neurochem* 1976; **26**: 345–352.

Patočková J, Marhol P, Tůmová E et al. Oxidative stress in the brain tissue of laboratory mice with acute post insulin with hypoglycemia. *Physiol Res* 2003; **52**: 131–135.

Pramming S, Thorsteinsson B, Bendtson I, Binder C. Symptomatic hypoglycaemia in 411 type 1 diabetic patients. *Diabet Med* 1991; **8**: 217–222.

Preston RJ, Bishop GA, Kitai ST. Medium spiny neuron projection from the rat striatum: an intracellular horseradish peroxidase study. *Brain Res*. 1980; **183**: 253–263.

Raivich G, Bohatschek M, Kloss CUA, Werner A, Jones LL, Kreutzberg GW.

Neuroglial activation repertoire in the injured brain: graded response, molecular mechanisms and cues to physiological function. *Brain Res Rev* 1999; **30**: 77–105.

Rovet JF, Ehrlich RM. The effect of hypoglycemic seizures on cognitive function in children with diabetes: A 7-year prospective study. *J Pediatr* 1999; **134**: 503–506.

Salter MW, Stevens B. Microglia emerge as central players in brain disease. *Nat Med* 2017; **23**: 1018–1027.

Sandberg M, Butcher SP, Hagberg H. Extracellular overflow of neuroactive amino acids during severe insulin-induced hypoglycemia: in vivo dialysis of the rat hippocampus. *J Neurochem* 1986; **47**: 178–184.

Schaefer PW, Grant PE, Gonzalez RG. Diffusion-weighted MR imaging of the brain. *Radiology* 2000; **217**: 331–345.

Stence N, Waite M, Dailey ME. Dynamics of microglial activation: a confocal time-lapse analysis in hippocampal slices. *Glia* 2001; **33**: 256–266.

Suh SW, Garnier P, Aoyama K, Chen Y, Swanson RA. Zinc release contributes to hypoglycemia-induced neuronal death. *Neurobiol Dis* 2004; **16**: 538–545.

Taylor SE, Morganti-Kossmann C, Lifshitz J, Ziebell JM. Rod microglia: A morphological definition. *PLoS One* 2014; **9**: e97096.

ter Braak EW, Appelman AM, van de Laak MF, Stolk RP, van Haeften TW, Erkelens

DW. Clinical characteristics of type 1 diabetic patients with and without severe hypoglycemia. *Diabetes Care* 2000; **23**: 1467–1471.

Thrane AS, Thrane VR, Nedergaard M et al. Drowning stars: reassessing the role of astrocytes in brain edema. *Trends in Neuroscience* 2014; **37**: 620–628.

Traynelis SF, Wollmuth LP, McBain CJ et al. Glutamate receptor ion channels: structure, regulation, and function. *Pharmacol Rev* 2010; **62**: 405–496.

Ünal-Çevik I, Kılınç M, Gürsoy-Özdemir Y, Gurer G, Dalkara T. Loss of NeuN immunoreactivity after cerebral ischemia does not indicate neuronal cell loss: a cautionary note. *Brain Res* 2004; **1015**: 169–174.

Wirenfeldt M, Clare R, Tung S, Bottini A, Mathern GW, Vinters HV. Increased activation of Iba1+ microglia in pediatric epilepsy patients with Rasmussen's encephalitis compared with cortical dysplasia and tuberous sclerosis complex. *Neurobiol Dis* 2009; **34**: 432–440.

Won SJ, Kim JH, Yoo BH et al. Prevention of hypoglycemia-induced neuronal death by minocycline. *J Neuroinflammation* 2012; **9**: 225.

Wyatt-Johnson SK, Herr SA, Brewster AL. Status Epilepticus triggers time-dependent alterations in microglia abundance and morphological phenotypes in the hippocampus. *Front Neurol* 2017; **8**: 700.

Yang X, Hamner MA, Brown AM et al. Novel hypoglycemic injury mechanism: N-Methyl-D-Aspartate receptor mediated white matter damage. *Ann Neurol* 2014; **75**: 492–507.

Ziebell JM, Taylor SE, Cao T, Harrison JL, Lifshitz J. Rod microglia: elongation, alignment, and coupling to form trains across the somatosensory cortex after experimental diffuse brain injury. *J Neuroinflammation* 2012; **9**: 247.